

# Chapter 9

## Platinum-Group Element Deposits in Layered Intrusions: Recent Advances in the Understanding of the Ore Forming Processes

Bélinda Godel

**Abstract** The major deposits of platinum-group elements (PGE) of the Earth are associated with ultramafic and mafic igneous rocks. The bulk of current PGE production is extracted from narrow stratiform horizons referred to as reefs located in the lower to central portions of large layered intrusions and is dominated by the Bushveld Complex in South Africa. The PGE-mineralized horizons occur in most case as laterally continuous and uniform layers that can extend over hundreds of kilometres along strike. The origins of these extensive PGE-rich layers remain controversial and subject to debate. Over the past ten years, technological developments have allowed the acquisition of multidisciplinary dataset at spatial resolution, detection limits and precisions that were impossible to achieve in the past. The results obtained provide additional insights into the complexity of the ores and the variability both within and between different ore deposits and highlight the necessity of adapting (for each deposit) models of formation based on all of the information available. Models of formation of PGE-reefs need to consider and integrate the superimposition of both physical and geochemical processes, over a range of scales and over a wide range of temperatures.

**Keywords** PGE · Cumulates · Bushveld · Reef · Ultramafic

### Introduction

The platinum-group elements (PGE: Pt, Pd, Ir, Os, Rh and Ru) are highly-siderophile elements used in a range of applications including the automobile industry (e.g. autocatalysts), jewellery, medicine (e.g. pacemakers, dental alloys, cancer treatments) and the high technology sector (e.g. electric contacts and production of glass fibres). Over the past ten years, the demand for PGE has continued to increase, resulting in a boom in mineral exploration to find new resources. Currently, most of the

---

B. Godel (✉)

ICSIRO Mineral Resources Flagship, 26 Dick Perry Avenue,  
Kensington, WA 6151, Australia  
e-mail: belinda.godel@csiro.au

© Springer Science+Business Media Dordrecht 2015  
B. Charlier et al. (eds.), *Layered Intrusions*, Springer Geology,  
DOI 10.1007/978-94-017-9652-1\_9

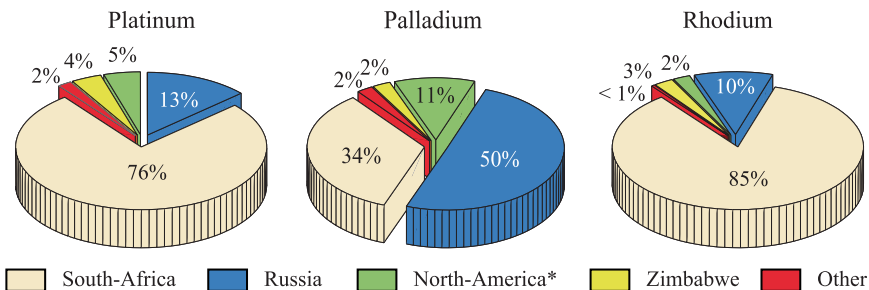


**Fig. 9.1** Average world's platinum-group elements supply by country for the period 2007–2011. Data are extracted from Johnson–Mattheys (2011) and presented by commodity

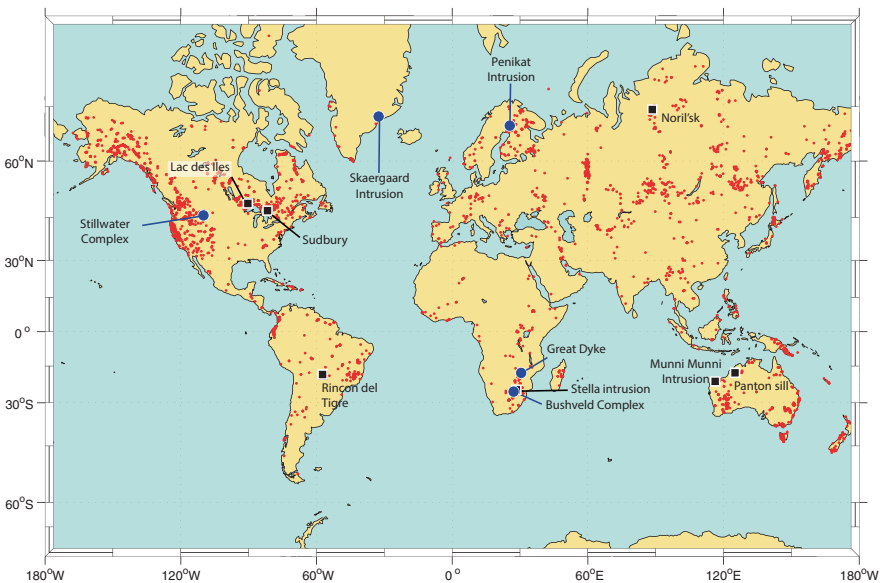


**Fig. 9.2** World's map showing the main economic PGE-deposits and PGE occurrences in mafic and ultramafic rocks. The locations of PGE deposits and occurrences are extracted from the USGS PGE–Ni–Cr deposit and occurrence bibliographic database (Causey et al. 2009)

world's supply of PGE is provided by only few countries (Johnson-Matthey 2011): South Africa, Zimbabwe, Russia, Canada and the U.S.A (Fig. 9.1). There are many occurrences of PGE in the world (Fig. 9.2) with three main groups of mineralization (Cawthorn et al. 2005; Maier 2005; Naldrett 2004) occurring as: (i) stratiform PGE mineralization within mafic-ultramafic intrusions (referred to as “reefs”); (ii) a by-product of major Ni–Cu sulfide deposits and; (iii) placers.

The major deposits of PGE are associated with ultramafic and mafic igneous rocks (e.g. layered and unlayered intrusions and zoned ultramafic complexes) that usually occur in tectonically stable areas (Eales and Cawthorn 1996; Maier and Groves 2011; Wager and Brown 1968). Platinum-group element mineralization has

been identified in various rock types and stratigraphic levels in layered intrusions of any age, size and origin (Maier 2005). However, most of the PGE resources on Earth are currently mined from narrow stratiform reefs located in the lower to central portions of large layered intrusions. These intrusions are Archean to early Proterozoic in age and have parental magmas with magnesian compositions (e.g. the Bushveld Complex in South Africa (Chap. 12), the Great Dyke in Zimbabwe (Oberthür 2002; Wilson and Tredoux 1990) and the Stillwater Complex in the U.S.A (McCallum et al. 1980; Raedeke and McCallum 1984, Zientek, 2002). Other PGE-rich zones have been observed in the upper portions of layered intrusions and are associated with sulfur-poor and Fe–Ti-rich rocks (e.g. Skaergaard intrusion in West Greenland (Andersen et al. 1998; Nielsen 2001), the Stella intrusion in South-Africa (Maier et al. 2003), the Rio Jacaré intrusion in Brazil (Sa et al. 2005), the Rincon del Tigre in Bolivia (Prendergast 2000), the Sonju Lake intrusion in the Duluth Complex in the U.S.A (Miller et al. 2002) or the Kotelainen intrusion in Finland (Mutanen 1997)). Platinum-group element mineralization observed in the upper part of the intrusion is in most cases uneconomic with only a few exceptions (e.g. the Stella and the Skaergaard intrusions). Significant PGE mineralization is also observed in poorly-layered (e.g. Noril'sk–Talnakh in Russia, (Arndt et al. 2005)) or unlayered intrusions (e.g. the Lac des Iles intrusion in Canada (Lavigne and Michaud 2001)).

Several schools of thoughts for the origin of PGE mineralization in layered intrusions have emerged over the years, with some authors suggesting that: (i) the PGE crystallize directly from the magma in the form of platinum-group minerals (PGM) that accumulate on the crystal pile (Hiemstra 1979); (ii) the PGE were collected by a sulfide liquid that segregated from the magma and accumulated on the cumulate pile (Campbell and Naldrett 1979; Campbell et al. 1983; Naldrett et al. 1986); or (iii) the PGE were collected by a fluid migrating upwards through the cumulate pile during compaction (Boudreau 1999; Boudreau 2008; Boudreau and Mc Callum 1992b; Willmore et al. 2000). Although research on the PGE deposits has increased in the past twenty years, the processes that controlled the PGE enrichment in layered intrusions remain controversial and vigorously debated as none of the models named above have successfully explained the structure, petrology, geochemistry and mineralogy of the PGE-rich horizons (e.g. Cawthorn et al. 2005; Mungall and Naldrett 2008).

Recent technological developments (e.g. laser ablation inductively coupled mass spectrometry (LA-ICP-MS), high-resolution X-ray computed tomography, isotope-ratio mass spectrometers, or automated scanning-electron microscope) have allowed the acquisition of multi-disciplinary datasets at spatial resolution, detection limits and precisions that were impossible to achieve in the past. These new results have provided additional insight into the genesis of the PGE deposits. This contribution presents short descriptions of selected layered intrusions hosting significant PGE mineralization and reviews the main type of PGE deposits observed. This is followed by a discussion on the residency of PGE in the rocks and the processes that may occur during ore genesis, from the partial melting of the Earth's mantle to the post-cumulus redistribution of the PGE.

## Geology of Selected Layered Intrusions

Current production and future reserves of Pt, Pd and Rh are overwhelmingly dominated by deposits associated with the Bushveld Complex in South Africa (Fig. 9.1). Consequently, a large proportion of the research effort in the last ten years has been undertaken to provide additional insights into the genesis of economic PGE-reefs focussed on the Bushveld Complex. In comparison, a relatively limited number of studies published in the literature have focussed on the genesis of other significant PGE-deposits hosted within layered intrusions (e.g. the Great Dyke, the Stillwater Complex, the Penikat or the Skaergaard intrusions). The geology and the petrography of these intrusions are summarized below to provide a basis for the descriptions of mineralization types and characteristics of PGE reefs occurring in these layered intrusions.

### *Bushveld Complex*

The Bushveld Complex in South-Africa (Eales and Cawthorn 1996; Chap. 12; Wager and Brown 1968) was intruded at  $2057.7 \pm 1.6$  Ma (Olsson et al. 2010) into the Kaapvaal craton subparallel to the sedimentary layering of the Transvaal Supergroup (Fig. 9.3). It is by far the largest layered intrusion in the world (Eales and Cawthorn 1996) and extends over 450 km east-west and 350 km north-south. The ultramafic and mafic rocks of the Bushveld Complex are referred to as the Rustenburg Layered Suite (South African Committee For Stratigraphy 1980). The 6.5–8.7 km thick Rustenburg Layered Suite has undergone little deformation or metamorphism after its solidification (Eales et al. 1993). It comprises four outcropping areas referred to as limbs (Fig. 9.3): the western limb, eastern limb, the far western limb, the northern limb. A fifth limb (referred to as “the Bethal limb”, in the south crops out as a small inlier of granophyre and comprises only Upper Zone stratigraphy that is covered by Karoo sediments (Buchanan 1979; Kruger 2005). Seismic and gravity data suggested that the Eastern and Western Limbs originally formed a continuous intrusion (Cawthorn and Webb 2001; Cole et al. 2014; Webb et al. 2004). The northern limb is separated from the other limbs by the Thabazimbi–Murchison regional fault zone that formed around 2.9 Ga and is a terrane boundary that separates the southern Archean crust and lithospheric mantle of the Kaapvaal Shield from the Pietersburg Block to the north (McDonald and Holwell 2011 and references therein). The ultramafic and mafic rocks of the Rustenburg Layered Suite have been sub-divided on the basis of cumulus mineral assemblages into five major zones (South African Committee for Stratigraphy, 1980): the Marginal zone mainly formed of fine-grained norite; the Lower Zone consisting of cyclic units of orthopyroxenite, minor harzburgite, and minor chromitite); the Critical Zone formed by pyroxenite, norite, anorthosite and chromitite; the Main Zone consisting mainly of gabbro-norite and; the Upper Zone formed by anorthosite, diorite and magnetitite (Fig. 9.3 and Fig. 9.4). Although there are a number of layers enriched in PGE within the intrusion (Barnes and Maier 2002a; Naldrett 2004) only three are sufficiently enriched in PGE, and continuous enough, to be called reefs: the Upper

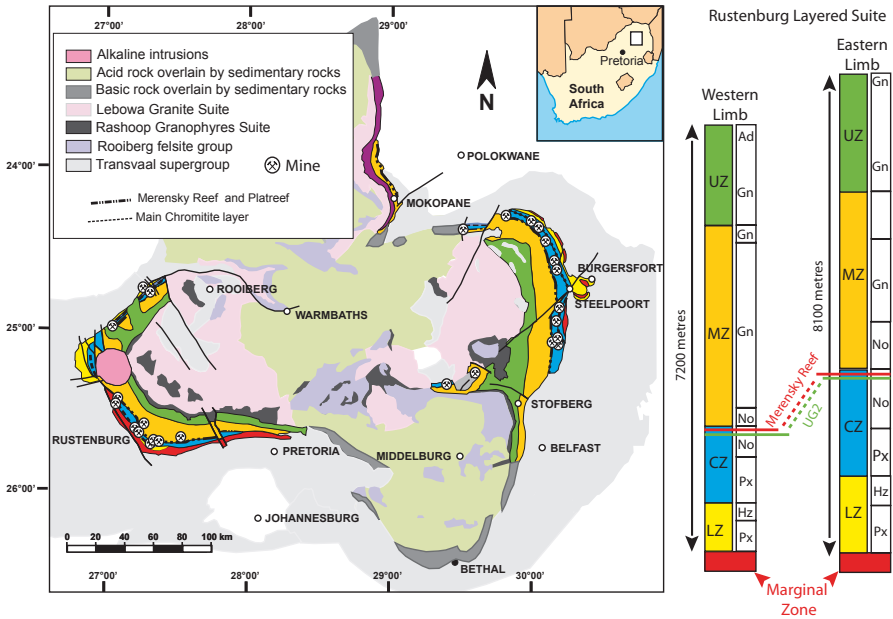


**Fig. 9.3** Simplified geological map of the Bushveld Complex (South Africa) and stratigraphy of the Rustenburg Layered Suite. The geological map is adapted from Von Gruenewaldt 1979 and the stratigraphy for the Eastern and Western Limbs are modified after Cawthorn et al. (2005). LZ Lower Zone; CZ Critical Zone, MZ Main Zone; UZ Upper Critical Zone; Px pyroxenite, Hz harzburgite; No Norite; Gn gabbronorite; AD Apatite Diorite

Group Chromitite 2 (UG-2), the Merensky Reef, and the Platreef (Fig. 9.3). These reefs represent the world’s three largest PGE horizons (Cawthorn 1999; Naldrett 2011; Naldrett et al. 2011a). The Platreef is situated at the base of the intrusion in the Northern Limb. In contrast, the UG-2 chromitite and the Merensky Reef are located in the upper part of the Critical Zone some 2 km above the base of the intrusion and crop out both in the Western and Eastern Limbs (Fig. 9.3).

### Stillwater Complex

The 2705±4 Ma old (Premo et al. 1990) Stillwater Complex is a layered ultramafic to mafic intrusion that is located in southwestern Montana in the U.S.A. (Fig. 9.5). The base of the Stillwater complex is in contact with middle to late Archean metasedimentary rocks, whereas the uppermost part of the complex is unconformably overlain by Phanerozoic sedimentary rocks. The original size of the complex is unknown as only a part (~44 km along its WNW strike length and ~6 km in thickness) of the complex is exposed along the Beartooth uplift (Page and Zientek 1985). Detailed descriptions of the petrography and stratigraphy of the complex were provided by Zientek et al. (2002 and references therein). To summarise, the layered rocks of the complex have been divided into five series (Fig. 9.5), from



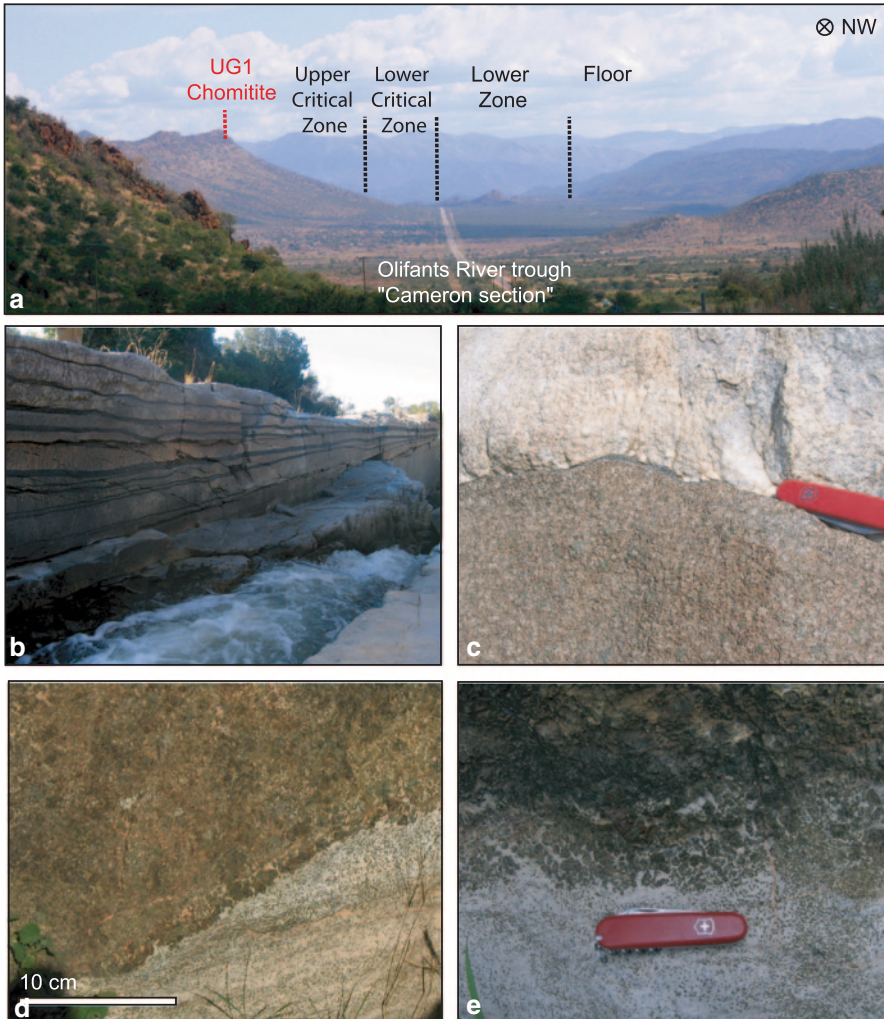


**Fig. 9.4** Photographs of field exposures showing different lithologies from the Bushveld Complex in South Africa, modified after Godel (2007). **a** View of lithological variations from the floor rocks to the Upper Critical Zone in the Olifants River Trough in the Eastern Limb of the Bushveld Complex. This section is referred to as the “Cameron section”. **b** Field exposure of the UG1 chromitite layers and interlayered plagioclase-rich rocks (Upper Critical Zone) at Dwars River, Eastern Limb of the Bushveld Complex. **c** Field exposure showing the contact between the Lower and the Upper Critical Zones (“Cameron Section”) with pyroxenite overlain by a thin layer of undulating chromitite overlain by anorthosite. **d** and **e** Examples of field outcrop of Merensky Reef in the Eastern Limb of the Bushveld Complex

bottom to top (Barnes and Naldrett 1986; McCallum et al. 1980; Page and Zientek 1985; Zientek et al. 1985): the Basal series consists of norites and bronzitites which contain minor amounts of base-metal sulfide minerals; the Ultramafic series is formed essentially of harzburgite and bronzitite, with minor chromite seams; the

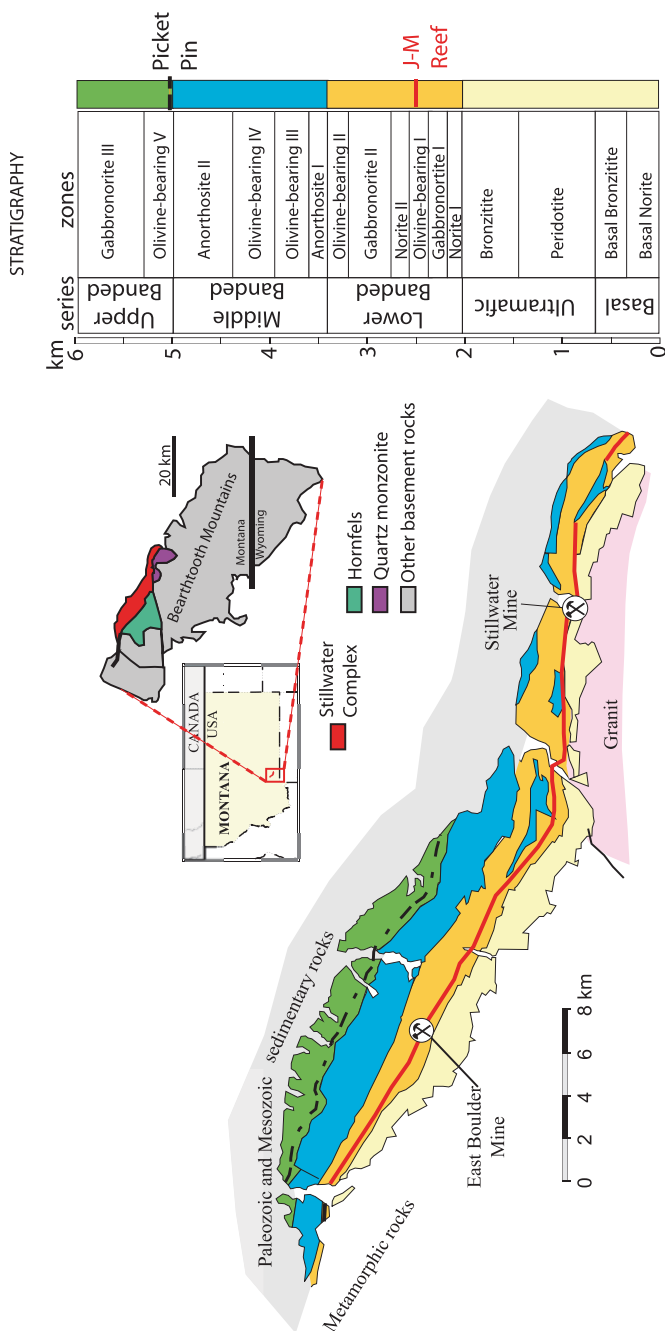


Fig. 9.5 Simplified geological map and stratigraphy of the Stillwater Complex (Montana). The geological map and the stratigraphy are modified after Zientek et al. (2002, 1985)

Lower, Middle, and Upper Banded series contain mainly norite, gabbro-norite, olivine gabbro-norite, troctolite and anorthosite. Several layers enriched in PGE are hosted within the complex, amongst them the Johns-Manville Reef (J-M Reef) and the Picket Pin deposit (Fig. 9.5). In contrast to the Bushveld Complex, the complex has been affected by several metamorphic and/or hydrothermal processes which have triggered alteration of the silicate and the sulfide minerals (Czamanske and Loferski 1996; Godel and Barnes 2008a; Godel and Barnes 2008b; Lechler et al. 2002; Page 1976; Polovina et al. 2004). The alteration commonly observed in the Stillwater Complex may notably be related to: (i) the initial crystallisation or cooling of the complex; (ii) the intrusion of quartz monzonite near the base of the complex (Nunes and Tilton 1971); (iii) the intrusion of mafic dikes and sills that crosscut the complex (Czamanske and Zientek 1985); (iv) greenschist facies metamorphism at 1.7 to 1.6 Ga (Nunes and Tilton 1971; Page 1977) or (v) the Cretaceous Rocky Mountains Laramide uplift (Polovina et al. 2004).

## ***Great Dyke***

The Great Dyke is a linear layered mafic-ultramafic intrusion that cuts across the Archean and early Proterozoic granites and greenstone belts of the Zimbabwe craton (Fig. 9.6). The  $2575.4 \pm 0.7$  Ma Great Dyke (Oberthür et al. 2002) has a highly elongated shape that makes it distinctly different to other large layered intrusion hosting PGE deposits such as the Bushveld and the Stillwater Complexes (Fig. 9.6). The Great Dyke is after the Bushveld Complex, the second largest single resource of PGE on Earth. The Great Dyke aligns along ~550 km in the NNE direction and is ~11 km wide (Worst 1960). It was emplaced as a series of initially isolated magma chambers that became linked at their highest levels during later stages of intrusion. The presence of satellite dykes located parallel to the intrusion are interpreted to reflect craton wide fractures that controlled the emplacement of the Great Dyke (Wilson and Prendergast 1989). The aspect ratio of the intrusion profoundly affected the rock types, layering style, the mineral composition and the mineralized ore bodies (Wilson 1996). Magma chambers and sub-chambers have been defined based on the style and continuity of the layering and the structure and comprise (Fig. 9.6) the North Chamber (subdivided into the Musengeiz, Darwendale and Sebakwe Subchambers) and the South Chambers (subdivided into the Selukwe and Wedza Subchambers). The Great Dyke stratigraphy (Fig. 9.6) is formally subdivided into a lower Ultramafic Sequence and an upper Mafic Sequence. The dynamic interplay between magma emplacement and crystallization gave rise to the succession of cyclic units within the Ultramafic Sequence (Wilson 1982). These cyclic units (Fig. 9.6) consist in the top of the sequence of a lower dunite or harzburgite layer overlain by a pyroxenite layer whereas, in the lower part the cyclic units are defined by chromitite layers intercalated within dunite (Wilson 1982). The PGE-mineralized zones (Oberthür 2011) are associated with the uppermost portion of the Ultramafic Sequence and those associated with sulfides represent by far the most important PGE concentrations (e.g. the Main Sulfide Zone).



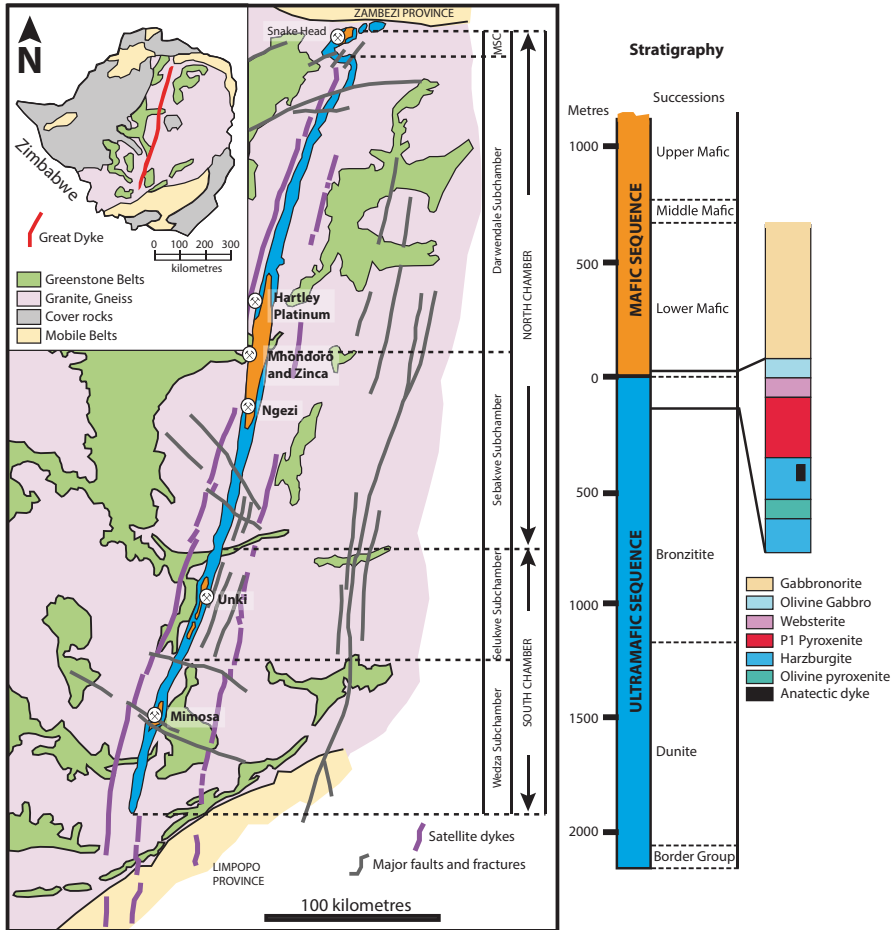
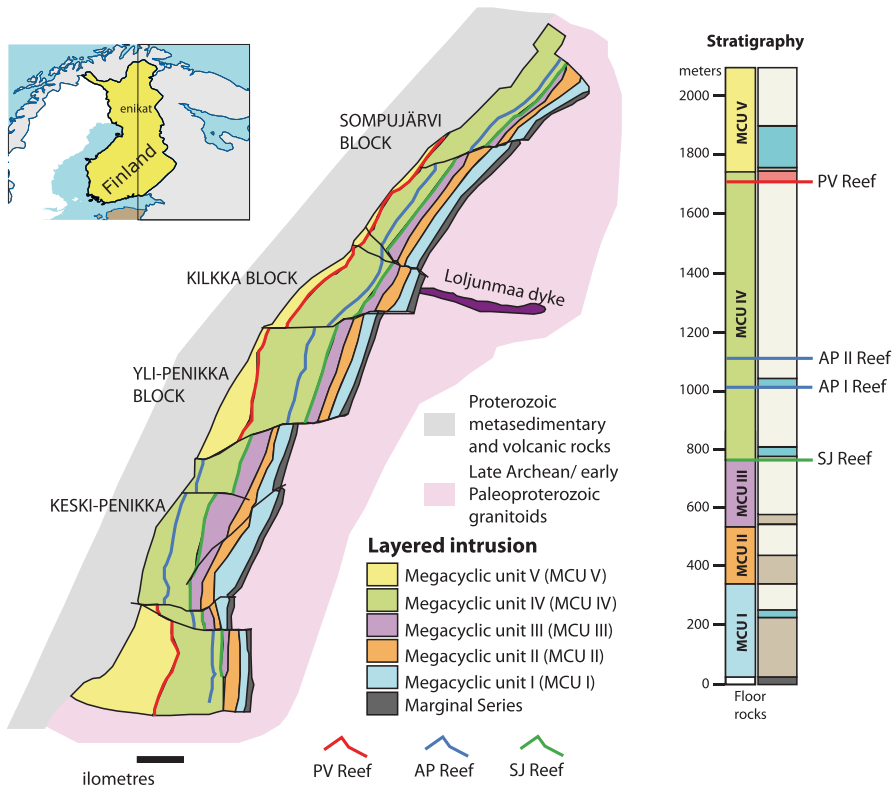


Fig. 9.6 Simplified geological map and stratigraphy of the Great Dyke of Zimbabwe. The geological map and the stratigraphy are modified after Wilson (1996) and Wilson and Prendergast (1989)

### Penikat Intrusion

The 2440 Ma old (Alapieti and Lahtinen 1986) Penikat intrusion belongs to a group of intrusions forming the 300 km long Tornio–Näränkävåara Belt that extends from east Sweden to south-west Finland. The Penikat intrusion is located ~70 km south of the Arctic Circle on the northern side of the Gulf of Bothnia (Fig. 9.7). The original shape of the intrusion is uncertain but its present surface is ~23 km long and 1.5 to 3.5 km wide. The original intrusion has been fragmented into five blocks (referred to as Sompujärvi, Kilka, Yli-Penikka, Keski-Penikka, and Ala-Penikka blocks, Fig. 9.7) during the Svecokarelidic orogeny. The mafic Loljunmaa Dyke located east of the Kilka block is co-magmatic to the intrusion and may represent a part of its feeder channel. The intrusion has been divided into three main



**Fig. 9.7** Simplified geological map and stratigraphy of the Penikat intrusion. The geological map is modified after Alapieti and Lahtinen (1986) and the stratigraphy is modified after Halkoaho et al. (1990)

units: the Marginal series, the Layered series and the granophyres (Alapieti and Lahtinen 1986). The Layered series consists of cyclic units of ultramafic, gabbroic, and anorthositic rocks which have further been divided, based on the variation in occurrence of cumulus minerals, into five megacyclic units referred to as Megacyclic Unit I to V (Fig. 9.7), from base to top. The basal units (Megacyclic units I to III) consist mainly of ultramafic rocks with minor mafic rocks where the upper units (Megacyclic units IV and V) are mainly formed by mafic rocks with minor ultramafic rocks (Alapieti and Lahtinen 2002). The PGE-rich mineralization is found in three distinct layers (SJ, AP and PV reefs) within the Megacyclic unit IV consisting, from bottom to top, of a 10 to 20 m thick layer of ultramafic cumulates overlain by a thick sequence of gabbroic and anorthositic cumulates (Alapieti and Lahtinen 1986). The Penikat Intrusion underwent complex deformation and metamorphism during the Svecokarelian Orogeny resulting in pervasive alteration of the cumulate rocks (Alapieti and Halkoaho 1995). The majority of the magmatic minerals have been altered to varying extents however augite grains are relatively well preserved (Alapieti and Halkoaho 1995).

## ***Skaergaard Intrusion***

The  $55.65 \pm 0.3$  Ma old (Hirschmann et al. 1997) Skaergaard Intrusion in East Greenland formed during the continental break up in the North Atlantic and was emplaced within the Tertiary East Greenland plateau basalts (Nielsen 1975). The intrusion is in a plan view  $\sim 11$  km long and  $\sim 8$  km wide (Fig. 9.8). The intrusion was originally interpreted to have formed by single event of magma injection into a magma chamber that crystallized and fractionated under generally closed-system conditions (McBirney 1996; Wager and Brown 1968). Holness et al. (2007) showed that several pulses of tholeiitic magmas were involved in the formation of the Skaergaard Intrusions and that intrusion cooled in a closed system after the magmas had homogenised into the chamber. The internal structure of the intrusion is divided into three series: the Layered Series (LS), the Marginal Border Series (MBS) and the Upper Border Series (UBS). Details of the stratigraphy, petrography and geochemistry of the intrusion are detailed in Tegner et al. (this volume) and are not repeated here. Palladium and gold mineralization are observed in the uppermost part ( $\sim 100$  m) of the Middle Zone (Andersen et al. 1998; Holwell and Keays 2014; Nielsen 2001). This stratiform group of layers rich in Pd and Au is referred to as the Platinova Reef (Bird et al. 1991).

## **Characteristics of the Different Deposit Types**

Platinum-group element mineralization classification have mainly been proposed based on the types of parental magmas from which the rocks crystallized (Naldrett 2004) or based on the stratigraphic setting of the mineralization and the rock types they are associated with (Maier 2005; Maier et al. 2013). Based on a simplified version of Maier's (2005) classification, the PGE-deposits associated with layered intrusions can mainly be classified into: (i) "Contact-type" PGE mineralization; (ii) PGE-mineralization associated with large chromitite layers at or near the base of macrorhythmic cycles; (iii) PGE-mineralization located in the lower- to middle part of layered intrusions and; (iv) PGE-mineralization located in the upper part of layered intrusions and associated with Fe-Ti oxide-rich rocks (Fig. 9.9).

### ***"Contact-Type" PGE-Mineralization***

The "contact-type" PGE mineralization owes its name to its location at or near the base or the sidewall of layered intrusions (Fig. 9.9). The mineralized zones are characterised by the presence of disseminated to massive base metal sulfides. Deposits of this type comprise the Platreef of the Bushveld Complex in South Africa (McDonald and Holwell 2011 and references therein) layered intrusions in northern Finland such as the Portimo complex (Alapieti and Lahtinen 2002), and the Feodorov-Panski intrusion in Russia (Dubrovsky and Rundqvist 2009). Typically,

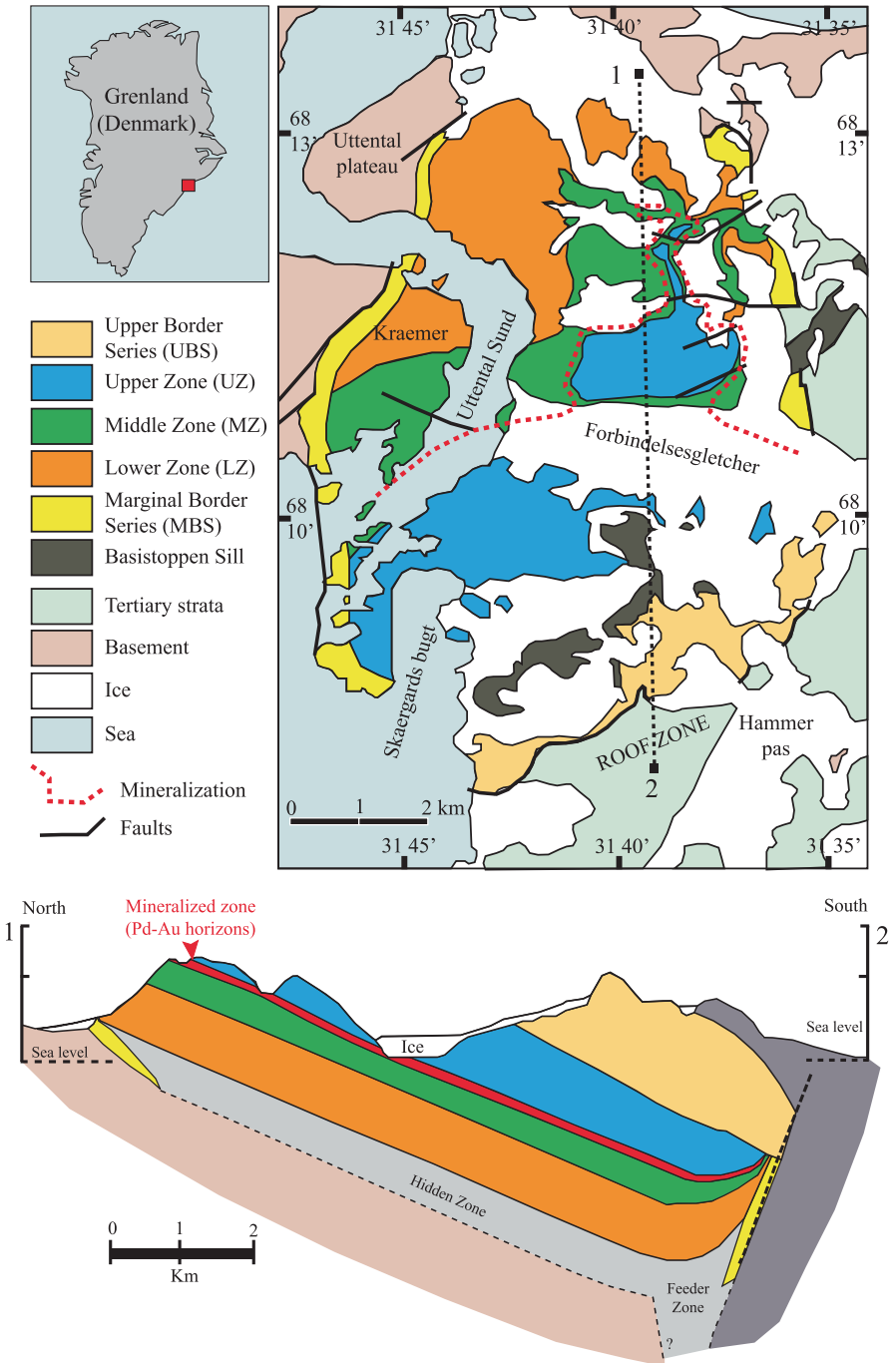


**Fig. 9.8** Simplified geological map and stratigraphy of the Skaergaard intrusion (East Greenland). The geological map (a) and the cross-section are modified after Wager and Brown (1968) and Nielsen (2004)

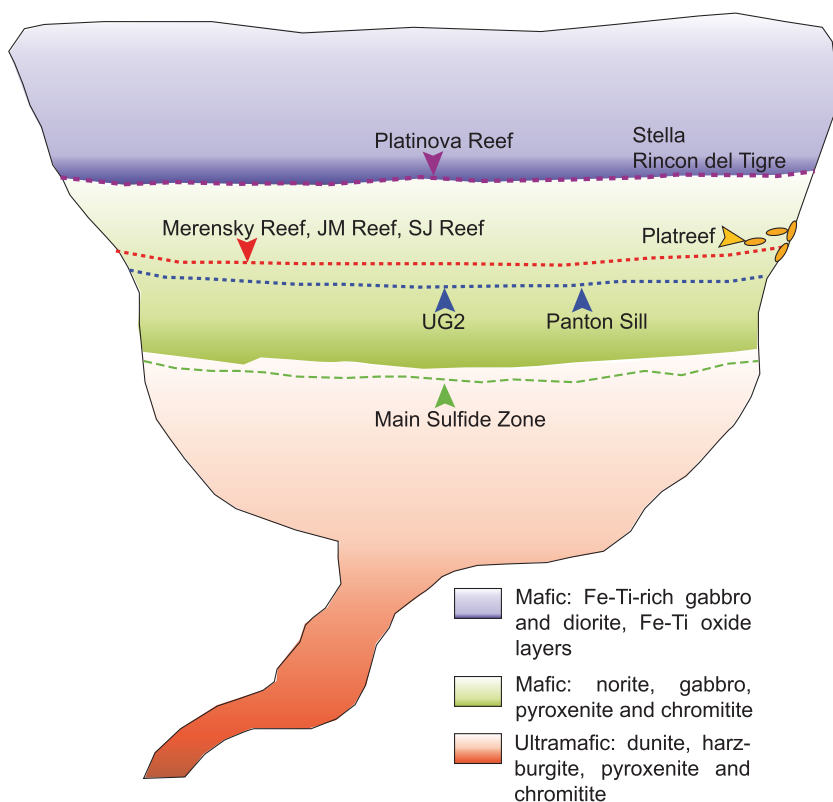


**Fig. 9.9** Schematic diagram showing the location of selected PGE-horizons in ultramafic-mafic layered intrusions. The figure is modified after Maier (2005)

the sulfide abundances are higher than other PGE reef types with proportions commonly averaging 5 to 10 volume percent. The sulfides are in most cases associated with heterogeneous mafic rocks and less commonly with ultramafic rocks except for the Platreef. The textures of the host rocks vary widely in terms of mineral abundances and crystal size and are referred to as “taxitic” or “variably textured” rocks. Xenoliths of the country rocks and veins of felsic rocks are commonly observed. Although the base metal sulfides are more abundant, the platinum-group element tenors are usually lower (typically in the order of 10’s ppm combined PGE) than those observed in reefs located in the middle portion of the intrusions.

The Platreef of the Bushveld Complex (due to its large size and attractive metal tenors) is currently the only contact-type PGE mineralization mined. The Platreef is defined as “a lithologically variable unit dominated by pyroxenite, which is irregularly mineralized with PGE, Cu and Ni, between the Transvaal metasedimentary footwall or the Archean basement and the overlying Main Zone gabbronorite” (Kinnaid et al. 2005; Manyeruke et al. 2005; McDonald and Holwell 2011; Yudovskaya et al. 2012). The mineralization is hosted within vari-textured pyroxenites, norites and gabbros with rare peridotites and chromitites. The reef thickness (10 to 400 m

thick) varies from south to north with largest thickness observed in the south. Its overall geometry appears to be controlled by irregular floor topology. The mineralized zone is relatively enriched in sulfur compared to other PGE-reef deposit. Sulfide minerals may reach >30 modal percent over several meters in some intersections. The sulfides are mainly composed of pyrrhotite, with lesser amounts of pentlandite, chalcopyrite and minor pyrite. The massive sulfides are mostly localized towards the contact with metasedimentary rocks of the footwall. Disseminated to net-textured sulfides are associated with intergranular plagioclase or quartz feldspar symplectites and observed as interstitial phases between rounded orthopyroxenes. The Platreef (Fig. 9.10) differs from the UG2 chromitite and the Merensky Reef in terms of thickness (from few centimetres to several tens of meters), PGE grade (lower, ~3 ppm Pt + Pd + Rh), Pt/Pd ratios vary from 0.2 to 1 and higher Cu and Ni (0.1–0.25% and 0.15–0.36%, respectively). The cumulate rocks of the Platreef are enriched in incompatible trace elements and have compositions distinct from the cumulate rocks from the Bushveld Complex. The rocks are also enriched in initial Sr,  $\epsilon$ Nd and  $\gamma$ Os isotopes and exhibit heavy S isotopic signatures suggesting crustal contamination (Barnes and Maier 2002a; Holwell et al. 2007; Penniston-Dorland et al. 2008). Recent, multi-sulfur isotope analysis (Sharman et al. 2013) indicated that a restricted stratigraphic horizon in the Platreef footwall (the Deutschland formation) contributed to the crustal sulfur isotopic signature of the ore. The addition of crustal sulfur lead to an apparent dilution of pre-existing PGE-rich sulfide melt (Sharman et al. 2013).

### ***PGE-Mineralization Associated With Large Chromitite Layers***

The enrichment of chromitites in Ir, Os and Ru (referred to as IPGE) is almost universal whereas enrichment in the other PGE, Pt, Pd and Rh (referred to as PPGE) are rarer. Chromitite layers observed in layered intrusions are usually enriched in all PGE compared to their silicate hosts (Hiemstra 1979; Lee and Parry 1988; Naldrett et al. 2011b; Teigler and Eales 1993; Von Gruenewaldt 1986). Another example is the sub-economic Panton Sill in Western Australia (Fig. 9.2). All chromitite layers of the Bushveld Complex are enriched in PGE with concentrations varying from 0.1 to 40 ppm. However, to date only one layer is currently of grade sufficient to be mined, the UG-2 chromitite. It is the second stratiform chromitite layer within the upper group of chromitite layers (Upper Critical Zone). The UG-2 sequence (60 to 120 cm thick) consists of thick chromitite overlying a pegmatoidal feldspathic pyroxenite and, more rarely anorthosite that extends over several hundred kilometres of strike length (Davey 1992). The chromite content varies between 60 to 90 modal percent with Cr/Fe ratios of the chromites ranging from 1.26 to 1.4 (Lee 1996 and references therein; Mondal and Mathez 2007; Naldrett et al. 2011b). The UG-2 contains major PGE-mineralization that represents the largest PGE resource in the world (Cawthorn et al. 2005; Lee 1996; Mungall and Naldrett 2008). The PGE concentrations average 5 ppm with zones hosting up to 10 ppm (Gain 1985; Hiemstra 1986; Maier and Barnes 2008; McLaren and De Villiers 1982; Naldrett et al. 2011b; Von Gruenewaldt 1986). The PGE (Figs. 9.10 and 9.11) tend to be more



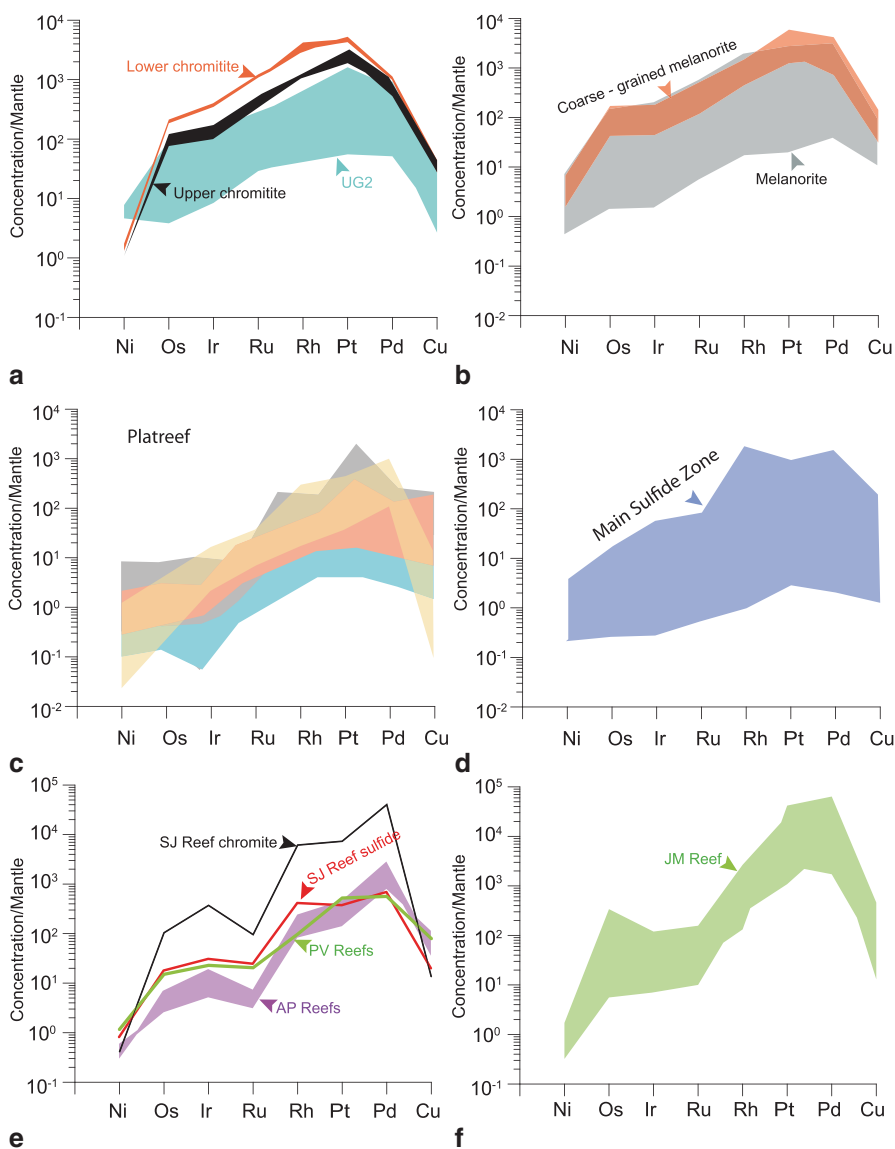


**Fig. 9.10** Whole-rock base-metal and platinum-group element concentrations from various PGE deposits represented as mantle-normalized spectra **a** Base-metal and platinum-group element concentrations of chromitite layers in the Merensky Reef (Lower and Upper chromitites) and the UG2 chromitite. The data are extracted from Godel et al. (2007), Maier and Barnes (2008), Barnes and Maier (2002b). **b** Base-metal and platinum-group element concentrations of coarse-grained (i.e. pegmatoidal) melanorite and melanorite from the Merensky Reef. The data are extracted from Godel et al. (2007), Barnes and Maier (2002b), Naldrett et al. (2009b) and Osbahr et al. (2013). **c** Base-metal and platinum-group element concentrations of pyroxenite from various localities within the Platreef. The data are extracted from Holwell and McDonald (2006, 2007) and Manyeruke et al. (2005). **d** Base-metal and platinum-group element concentrations across the

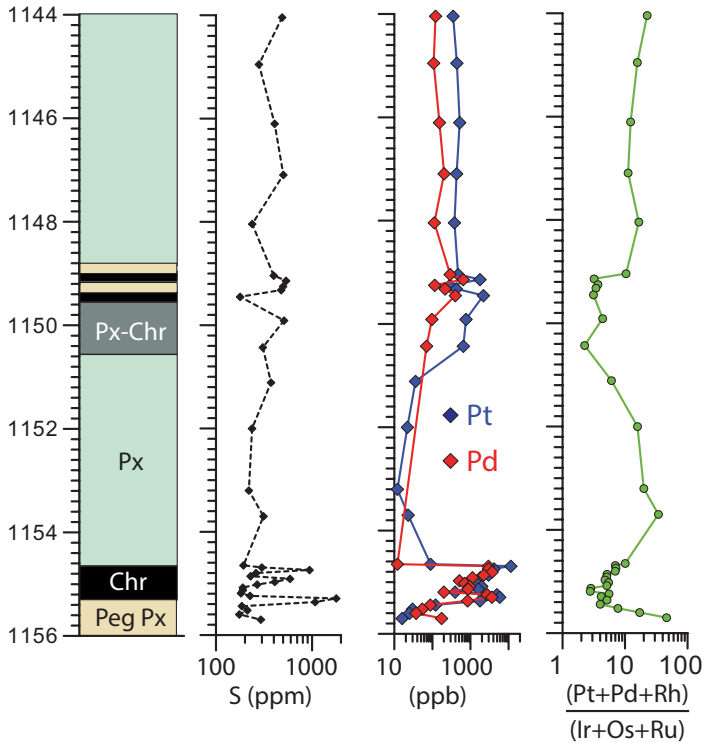


**Fig. 9.11** Stratigraphic variation of sulfur, PGE and base-metal concentration across the UG2 chromitite layer. The data are extracted from Maier and Barnes (2008). *Chr* chromitite; *Peg Px* Pegmatoidal pyroxenite and *Px* pyroxenite

concentrated towards the base and the upper contact of the layer (Maier and Barnes 2008; Von Gruenewaldt 1986). The sulfur concentration within the chromitite is less than 0.1 weight percent in most cases (Barnes et al. 2009; Maier and Barnes 2008) with exceptional sulfide abundance of up to 2.5 volume percent observed the Messina Mine (Von Gruenewaldt et al. 1990). Cawthorn et al. (2005) reported that the Pt/Pd ratios are significantly different from the Eastern to the Western Limb. However, no systematic variations in Pt/Pd ratios have been observed between the Northwest and Eastern Limbs (Naldrett et al. 2011b).

Main Sulfide Zone of the Great Dyke. The data are extracted from Wilson and Prendergast (2001). **e** Base-metal and platinum-group element concentrations in mineralized horizons from the Penikat intrusion in Finland. The data are extracted from Alapieti and Lahtinen (2002). **f** Base-metal and platinum-group element concentrations in the JM-Reef of the Stillwater Complex. The data are extracted from Godel and Barnes (2008b) and Barnes and Naldrett (1986). The coloured areas represent the range of concentrations observed. The concentrations have been normalized to the primitive mantle values from McDonough and Sun (McDonough and Sun 1995)

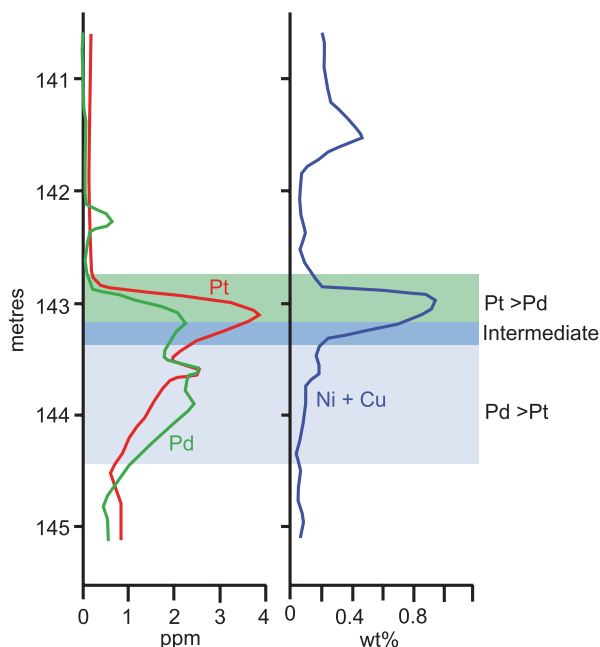
### ***PGE-Reef Types Located in the Lower to Middle Parts of Layered Intrusions***

Platinum-group element rich mineralization may occur in the lower part (<1000 m above the base) of layered intrusions. Deposits of this type are usually characterized by the presence of tens to hundreds of meters of disseminated base metal sulfides with sulfide abundances usually less than 5 volume percent. The base metal sulfides (in most case pyrrhotite, pentlandite and chalcopyrite) are hosted within peridotites and pyroxenites. Deposits of this type include the Santa Rita zone within the Mirabela intrusion (Barnes et al. 2011), the Kevitsa intrusion in Finland, and the Kapalagulu intrusion in Tanzania (Maier et al. 2008), and tend to have low PGE tenors. Platinum-group element mineralization observed higher (~1 to 2 km) in the stratigraphy are also characterized by the presence of disseminated base-metal sulfides (<5 volume percent). The PGE reefs usually occur in stratigraphic intervals where lithological and compositional changes occurred and where interlayering of ultramafic and mafic rocks is present (Barnes and Maier 2002a; Cawthorn et al. 2005). The host rocks may have various compositions from harzburgite, pyroxenite, troctolite, norite or anorthosite. Deposits of this type include the Merensky Reef of the Bushveld Complex, the JM Reef of the Stillwater Complex, the Main Sulfide Zone in the Great Dyke of Zimbabwe and the PGE reefs of the Penikat intrusion described below.

#### **The Main Sulfide Zone of the Great Dyke**

The Great Dyke of Zimbabwe hosts the world's second largest reserve of PGE (Oberthür 2011). The principal PGE resources of the Great Dyke are located in the Main Sulfide Zone (MSZ) and the Lower Sulfide Zone (LSZ) hosted within the P1 Pyroxenite of the uppermost Ultramafic Cyclic Unit (Fig. 9.6). The MSZ contains a higher abundance of sulfide and PGE than the LSZ and represent, by far the main PGE resource of the Great Dyke. The large majority of PGE resource (~75%) found in the MSZ is located in the Sebakwe and Darwendale Subchambers (Oberthür 2011). The PGE mineralization occurs in a narrow (1 to 2 m thick) zone towards the top of the ultramafic sequence. Disseminated base-metal sulfides composed of intergrowths of pyrrhotite, pentlandite, chalcopyrite and minor pyrite are hosted within mesocumulates composed mainly of orthopyroxene, augite, plagioclase, biotite, alkali feldspar and quartz (Wilson and Prendergast 2001). The base-metal sulfides represent 0.5 to 10 volume percent of the rock and occur as elongated blebs interstitial to silicate minerals. The MSZ is characterized by a particular distribution of the base-metal sulfide and the PGE referred to as "offset" reef in which the peaks both the Pt and Pd concentrations and the PGE and base metal sulfides are separated from each other stratigraphically (Fig. 9.12). The PGE mineralization has been defined into two main subzones with a lower Pd-rich (i.e. Pd > Pt) and an upper Pt-rich (i.e. Pt > Pd) subzones. The average PGE concentrations from various localities are presented in Fig. 9.10. Recent studies have shown that a large

**Fig. 9.12** Vertical distribution of PGE and base metals showing “Offset reef” of the Great Dyke of Zimbabwe. The data from a drillcore from the Mimosa mine and are extracted from Wilson and Prendergast (Wilson and Prendergast 2001) showing Pd and Pt-rich subzones



proportion of Pd and Rh are hosted in pentlandite whereas Pt is dominantly present in the form of platinum-group minerals (Oberthür 2011).

### Merensky Reef of the Bushveld Complex

The Merensky Reef is a narrow PGE reef that constitutes, after the UG-2 chromitite, the second largest PGE resource in the world. It occurs 15 to 400 m above the UG-2 chromitite (Lee 1996). The Merensky Reef lies at the base of a specific and very laterally persistent cyclic unit that contains thin basal chromitite layers (Vermaak 1976). The base of the Merensky Reef was used by some workers to define the boundary between the Upper Critical Zone and the Main Zone (Kruger 2005). The PGE- mineralization and the vertical succession are variable depending on the localities considered but are consistent across the entire intrusion in comprising a package of thin chromite stringers and locally pegmatoidal orthocumulate orthopyroxenite overlain by norite (Cawthorn 2002; Naldrett et al. 2009b; Viljoen 1999). Details of all the different reef types are presented in several studies (Kinloch 1982; Naldrett et al. 2009b; Viljoen 1999) and are not detailed in this contribution. The mineralized zone has a thickness that rarely exceeds 1 m with average PGE concentrations varying from 5 to 10 ppm and Pd/Pt ratios of  $\sim 0.6$  (Barnes and Maier 2002b; Cawthorn et al. 2005; Godel et al. 2007; Naldrett et al. 2009b; Wilson and Chunnett 2006). The so-called “normal” Merensky Reef (Fig. 9.13) consists, from the bottom upwards of (Barnes and Maier 2002b; Godel et al. 2006; Godel et al. 2008b; Naldrett et al. 2009b; Vukmanovic et al. 2013): (i) a footwall anor-

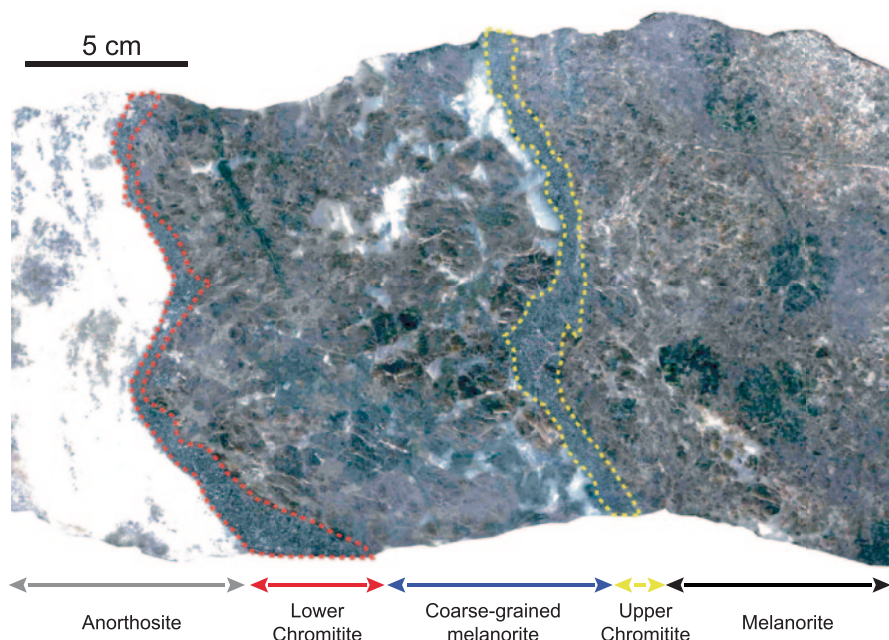


**Fig. 9.13** Typical normal Merensky Reef, Rustenburg Platinum Mine, Western Limb of the Bushveld Complex. Modified after Godel (2007)

thosite, pyroxenite or norite; (ii) a lower layer of chromitite that undulates at the centimetre scale and ranges from 2 to >40 mm in thickness containing euhedral to amoeboidal chromite crystals; (iii) a coarse-grained melanorite of varying thickness (from few centimetres to 10 m), with in some areas harzburgite and dunite; (iv) a thin (2 to 15 mm thick) upper chromitite layer containing euhedral chromite crystals overlain by (v) melanorite of thickness varying from 30 to 225 cm. Sulfide mineral proportions vary from 0.5 volume percent (in the chromitite layers) up to 10 volume percent in localized areas above the lower chromitite with average sulfide abundance of 3 volume percent over the reef (Barnes and Maier 2002b; Godel et al. 2007; Godel et al. 2008; Naldrett et al. 2009b). X-ray computed tomography and 3D image analysis reveal that in the pyroxenite, the sulfides are located at the boundaries of pyroxene and plagioclase crystals and form up to 10 cm interconnected networks. The sulfide networks fill paleovertical dilatancies formed during compaction, which facilitated the downward migration of sulfide liquid in the cumulate (Godel et al. 2006). These sulfide networks stop at the level of underlying chromitite layers where changes in sulfide wettability occur. The PGE concentrations are higher in the chromitite layers, vary at the centimetre scale and can reach locally 15 ppm total PGE (Figs. 9.14 and 9.10). Within both chromitite layers, high-resolution X-ray computed tomography combined with 3D quantitative image analysis and mineralogical analysis indicates that platinum group minerals occupy preferential sites at triple points between chromite, sulfide and silicate minerals at the edges of sulfide blebs (Godel et al. 2010). This observation implies that

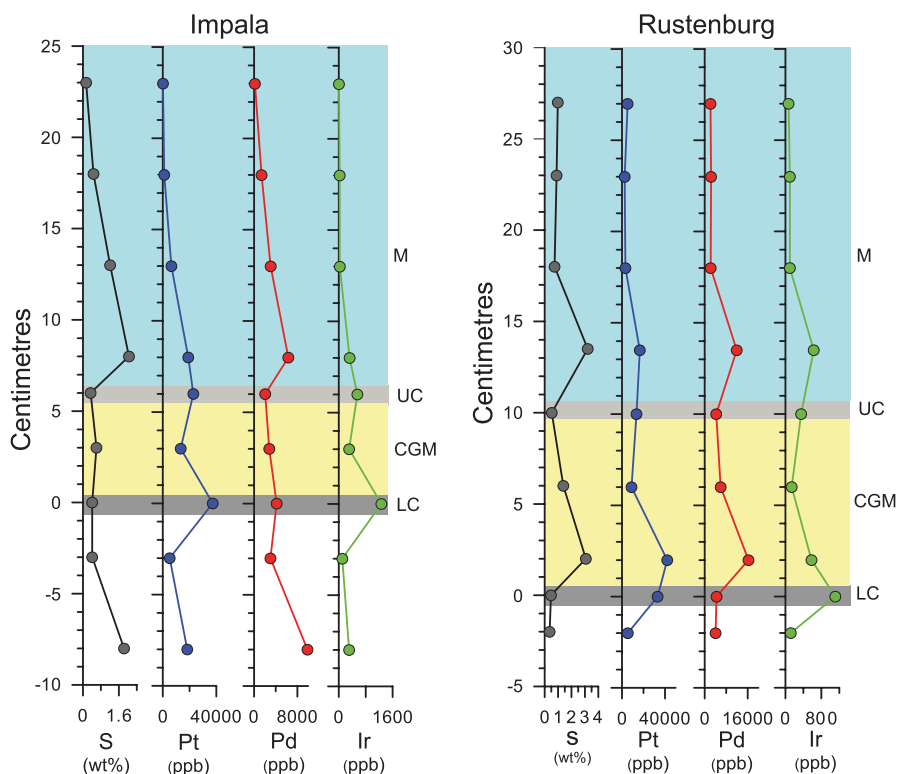


**Fig. 9.14** Stratigraphic variation of sulfur, PGE and base-metal concentration across the Merensky at the Impala and Rustenburg Platinum Mines. The data from Impala Mine are extracted from Barnes and Maier (2002b) and the data from the Rustenburg Pt Mine are from Godel et al. (2007). *LC* lower chromitite; *CGM* coarse-grained melanorite; *UC* upper chromitite and *M* melanorite

platinum-group minerals nucleated in preferred sites subsequent to accumulation of the sulfide droplets (Godel et al. 2010).

### J-M Reef of the Stillwater Complex

The Johns-Manville (J-M) Reef is the main PGE-rich layer within the complex and it is hosted within troctolite, olivine gabbronorite or anorthosite of the olivine-bearing cumulate zone I (OB-1) within the Lower Banded Series (Barnes and Naldrett 1986; Todd et al. 1982; Turner et al. 1985; Zientek et al. 2002 and references therein). Disseminated base metal sulfides (pyrrhotite, pentlandite, chalcopyrite and minor pyrite) locally represent 0.5 up to 5% by volume of the rock and form sulfide networks interconnected over distances of few centimetres. Where the cumulate rocks have been altered, secondary silicates (mainly chlorite, tremolite and actinolite) are closely associated with the sulfides, forming alteration haloes around them. In the altered olivine gabbronorite, the sulfides are altered to secondary magnetite



that form corona around the sulfides. Secondary chalcopyrite is also present and is associated with secondary silicates. The J-M Reef has the highest average Pt + Pd grade (~18 ppm with an average Pd/Pt ratio of 3) of all known PGE ore deposits (Zientek et al. 2002). The whole-rock concentration of Pd and Pt can reach values of several hundred ppm (Fig. 9.10) at the hand sample scale (Barnes and Naldrett 1986; Godel and Barnes 2008a; Godel and Barnes 2008b; Keays et al. 2012; Zientek et al. 2002). The Pd/Pt ratios are independent of the host rock type.

### **The SJ, AP and PV Reefs of the Penikat Intrusion**

The Sompujärvi Reef (referred to as SJ Reef) is located in the basal part of the Megacyclic Unit IV and is characterized by extremely low sulfide abundance and high PGE concentrations (up to tens of ppm PGE) associated with finely disseminated sulfides and chromite (Halkoaho et al. 1990). The Ala-Penikka Reefs (referred to as AP I and II Reefs) are observed ~200 to 400 m above the base of the Megacyclic Unit IV in the basal bronzitic portion and consist of narrow (0.4 to 1 m thick) PGE-rich mineralization associated with disseminated sulfides (4 volume percent). The AP I Reef is 2–70 cm thick and contains heterogeneous PGE concentrations associated with disseminated sulfides. The AP II Reef is found above the AP I Reef and exhibits similar characteristics. The Paasivaara Reef (referred to as PV Reef) is located at the transition between the Megacyclic Units IV and V (~700–1000 m above the AP Reefs) and is hosted within anorthosite (Alapieti and Lahtinen 1986; Huhtelin et al. 1990). Similarly to other reefs at Penikat, the PV PGE-mineralized zone is erratic in thickness and PGE concentration but contains the highest Pt/Pd ratios of all the reefs observed in the intrusion (Fig. 9.10). The PGE are associated with disseminated sulfides in the PV Reef (Alapieti and Lahtinen 1986; Huhtelin et al. 1990).

### ***PGE Reef Types in the Upper Parts of Layered Intrusions***

Occurrence of platinum-group element and gold mineralization have been described in the upper portion of layered intrusions (e.g. the Skaergaard Intrusion in west Greenland (Andersen et al. 1998), the Rio Jacaré complex in Brazil (Sa et al. 2005), the Sonju Lake and Birch Lakes intrusions in the Duluth complex in the U.S.A. (Miller et al. 2002), the Rincon del Tigre intrusion in Bolivia (Prendergast 2000), the Stella intrusion in South Africa (Maier et al. 2003), or the Kotalainen intrusion in Finland (Mutanen 1997)). In contrast to the other PGE-types, the mineralization is often hosted in gabbro-diorite and Fe–(Ti) oxide-rich layers. The deposits are relatively enriched in Cu, Pd, Au and Pt with considerably smaller Ru, Ir, Os concentrations. This is illustrated by the large Pd/Ir and Cu, Ni ratios of the rocks (e.g. average Pd/Ir ratios of ~150 and 250 for and Cu/Ni ratios of 2.45 and 3.122 for the Rio Jacaré and Stella intrusions, respectively). In most of the intrusions, the PGE grades are too low (typically 0.5 to 2 ppm) to be economic. The Skaergaard

and Stella intrusions contain higher grades (ca. 5 to 15 ppm) over thin interval and feasibility studies are under way potentially to mine the PGE and Au.

The Platinova Reef is associated with tens-of-meter scale modal layers referred to as the Triple Group, formed by oxide-rich tholeiitic gabbros (Wager and Brown 1968). The Reef occurs in repeated meter-thick layers of sulfide-poor gabbros located in the lower part of the Triple Group consisting of three conspicuous plagioclase-rich leuco-gabbro layers within plagioclase-pyroxene-oxide melanogabbros (Andersen et al. 1998; Nielsen et al. 2005). The Platinova Reef is inferred from compilation of drillcore data to comprise 8 continuous Pd-rich horizons, named from base to top: Pd5, Pd4b, Pd4a, Pd3b, Pd3a, Pd2b, Pd2a and Pd1 (Nielsen 2001). The PGE mineralization horizons are perfectly concordant with the layering in the host rocks and internal variations correlate throughout the intrusion (Nielsen et al. 2005). The number of Pd-enriched layers and the combined total PGE and Au contents increase toward the centre of the mineralization (Andersen et al. 1998; Holwell and Keays 2014; Nielsen et al. 2005). The main PGE reef (Pd5) of the Platinova Reef is a 4–5 m (at a cut off of 0.7 ppm) thick mineralized horizon with maximal grade reaching 5 ppm PGE (Nielsen et al. 2005). In contrast to other PGE reef types, the base-metal sulfides in the Pd5 layer are entirely dominated by bornite ( $\text{Cu}_5\text{FeS}_4$ ) with exsolution lamellae of chalcocite ( $\text{Cu}_2\text{S}$ ) and digenite ( $\text{Cu}_9\text{S}_5$ ). These Cu-sulfides represent less than 0.05 modal percent of the samples. In 3D, the Cu-rich sulfides (bornite  $\pm$  chalcocite assemblage) occur either as sub-spherical (sphericity  $>0.9$ ) globules that are mainly observed entirely enclosed within Fe–Ti oxides or as more irregular Cu-rich sulfide blebs that are either located at the boundaries between silicates (pyroxene or olivine) and Fe–Ti oxides or located between silicates grains (Godel et al. 2014). More than 75% (by volume of PGM) are associated with base-metal sulfides. Palladium, the main element that can potentially be mined, is almost entirely hosted by skargaardite (PdCu) (Rudashevsky et al. 2009). Most of the Skaergaardite (PdCu) occurs (in 3D) as globular to elongated grains found attached to subspherical (sphericity  $>0.9$ ) Cu-rich sulfide blebs enclosed within large ilmenite grains (Godel et al. 2014).

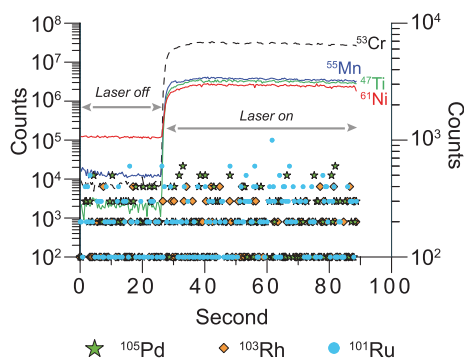
## Hosts of the Platinum-Group Elements

As described above, all the PGE-reefs currently mined consist of narrow mineralized zones associated with base-metal sulfides disseminated within silicate and/or chromite crystal matrices or chromitites containing trace amounts of sulfides. Over the past ten years, multi-disciplinary studies (e.g. X-ray computed tomography, whole-rock geochemistry, in situ mineral analysis by laser ablation ICP-MS, and the detailed analysis of platinum-group minerals and their textural characteristics) have been carried out on various reefs hosted within layered intrusions. The results of these studies have brought additional insights into the residency of the PGE in the mineralized rocks with important implications for ore genesis.

## Oxides

Chromitites in mafic-ultramafic layered intrusions are often enriched in PGE relative to their silicate host lithologies (e.g. Great Dyke, Bushveld Complex, Rum intrusion). Two mechanisms have been proposed to explain the relationship between chromite and the PGE and the Ir-group PGE (referred to as IPGE and comprising Ir, Os and Ru) in particular: (i) the IPGE could partition into chromite crystals and be present in solid solution or ii) the IPGE could exhibit low solubility in mafic magma and crystallise in the form of IPGE-rich minerals or alloys during chromite crystallization. The first hypothesis is based on experimental studies that have shown that Ir, Ru, Rh and Pd could partition into spinel phases (Brenan et al. 2012; Capobianco and Drake 1990; Capobianco et al. 1994; Righter et al. 2004; Sattari et al. 2002). Recently, homogeneous Ru laser ablation ICP-MS spectra in chromite from komatiites have been interpreted as evidence of partitioning of the IPGE in solid solution within natural chromite crystals (Locmelis et al. 2011; Pagé et al. 2012). Several laser-ablation ICP-MS analyses have been carried out on chromite crystals from the Merensky Reef of the Bushveld Complex (Ballhaus and Sylvester 2000; Godel et al. 2008; Osbahr et al. 2013), and on chromite and secondary magnetite grains of the J-M Reef of the Stillwater Complex (Godel et al. 2008), in order to test whether the PGE partitioned into natural spinel phases in sulfide-rich PGE-reef environments. The results of all of these studies indicate that none of the PGE are present in detectable (i.e. in the range of 10s ppb) amounts in chromite (Fig. 9.15) or secondary magnetite observed within the reefs. In these minerals, the PGE are only found as discrete PGE-rich phases mainly Pt-rich in the Merensky Reef (Ballhaus and Sylvester 2000; Godel et al. 2008; Osbahr et al. 2013), Pd-rich in the J-M Reef (Godel and Barnes 2008a) with minor Ru, Os, Ir (probably laurite) in both cases. Although to date no data are available for other deposit, it seems improbable that chromite and spinel in general contribute significantly to the PGE mass balance in PGE reefs.

**Fig. 9.15** Example of laser ablation spectra of chromite crystal from upper chromitite of the Merensky Reef of the Bushveld Complex showing the variation of selected platinum-group elements



## ***Base-Metal Sulfides***

Over the past ten years, the development of laser-ablation ICP-MS allowed the determination of trace element concentrations at ppb to ppm levels in base metal sulfides (pentlandite, pyrrhotite, chalcopyrite and pyrite) and provided a means for the evaluation of the contribution of base-metal sulfides to the overall PGE mass balance in PGE ore deposits. A large body of data now exists on the concentrations of PGE and semi-metals in sulfide minerals from different PGE-mineralization hosted within layered intrusions including the Merensky Reef (Ballhaus and Sylvester 2000; Godel et al. 2007; Osbahr et al. 2013); the Platereef (Holwell and McDonald 2006; Holwell and McDonald 2007; Hutchinson and McDonald 2008) and the UG2 (Osbaahr 2012) of the Bushveld Complex; the JM-Reef of the Stillwater Complex (Godel and Barnes 2008b); the Main sulfide Zone of the Great Dyke (Barnes et al. 2008); and the AP and PV reefs of the Penikat intrusions (Barnes et al. 2008).

In the Bushveld (Merensky Reef, Platereef and UG2) and Stillwater (JM Reef) Complexes, pentlandite is the main carrier of PGE in solid solution followed by pyrrhotite (Fig. 9.16a–d). In contrast, in the Great Dyke (Main Sulfide Zone) and the Penikat Intrusion (AP and PV reefs) pentlandite and pyrrhotite contain similar amounts of PGE in solid solution (Figs. 9.16e and f). In all cases, chalcopyrite is almost entirely devoid of PGE in solid solution (Fig. 9.16). Overall, the shape of mantle normalized metal patterns of pentlandite (Fig. 9.17) and pyrrhotite (Fig. 9.18) are comparable from one deposit to the other. Palladium is the principal PGE hosted in the base-metal sulfides with concentrations in pentlandite from the JM Reef reaching several weight percent (Cabri et al. 1984; Godel and Barnes 2008b; Polovina et al. 2004) as illustrated in Fig. 9.17. The contribution of pentlandite on the Pd budget in the whole-rock varies between reefs, with values reaching average of 75% in the Merensky Reef (Figs. 9.16a and b). Osmium, Ir, Ru and Rh concentrations in pentlandite (and to a lesser extent pyrrhotite) are broadly similar in the different reefs including the Merensky Reef chromitite layers and the UG2. The contribution of base-metal sulfide to the IPGE budget is smaller in the chromitite layers (e.g. UG2, Fig. 9.16c) than in sulfide-dominated PGE mineralization (Fig. 9.16). The similarity of IPGE patterns for all the deposits suggest that the processes that lead to the concentrations of these elements in the base-metal sulfides are comparable and would indicate that the concentrations have not significantly been influenced by post-magmatic processes such as alteration and metamorphism. Platinum concentrations in pentlandite and pyrrhotite are extremely low as illustrated by the strong negative anomalies observed on all the mantle-normalized metal patterns of pentlandite (Fig. 9.17) and pyrrhotite from the JM Reef (Fig. 9.18b). Only a small proportion (<5%) of the whole-rock Pt budget is accounted by the base-metal sulfides. Based on the results described above, it is clear that although PGE in the whole-rocks are correlated to their sulfur contents in most cases, base-metal sulfides are not the main host of PGE in the rocks.

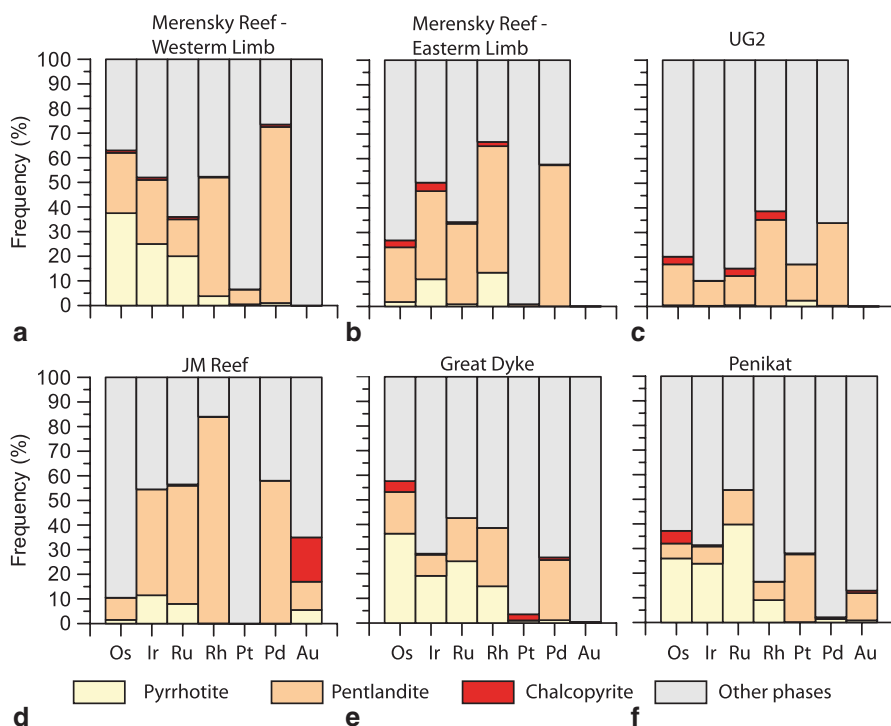


**Fig. 9.16** Average mass balance of platinum-group elements between whole-rock, base-metal sulfides and other phases in various PGE reefs. **a** Merensky Reef (Western Limb of the Bushveld Complex). The data are extracted from Godel et al. (2007) and Osbahr et al. (2013). **b** Merensky Reef (Eastern Limb of the Bushveld Complex). The data are extracted from Osbahr et al. (2013). **c** UG2. The data are extracted from Osbahr (2012). **d** JM Reef of the Stillwater Complex. The data are extracted from Godel and Barnes (2008b). **e** Main sulfide Zone of the Great Dyke. The data are extracted from Barnes et al. (2008). **f** AP and PV Reefs of the Penikat intrusion. The data are extracted from Barnes et al. (2008)

### Platinum-Group Minerals

The detailed LA-ICP-MS analysis and PGE-mass balances carried out on various deposits described above revealed that in a vast majority of cases, most of the PGE budget in the whole rock is controlled by platinum-group minerals (Fig. 9.16). The increased availability of scanning electron microscope (SEM), the development of SEM-based automated mineral liberation analyser (SEM-MLA), high-resolution X-ray computed tomography and image processing techniques have made it possible to constrain the location, composition, size and textural relationships in both 2D and 3D of the platinum-group minerals at the sample scales (Figs. 9.19 and 9.20). A large number of recent studies have reported platinum-group mineral (PGM) analyses for major PGE deposits (Barnes et al. 2008; Godel 2013; Godel and Barnes 2008a; Godel and Barnes 2008b; Godel et al. 2007; Godel et al. 2010; Holwell

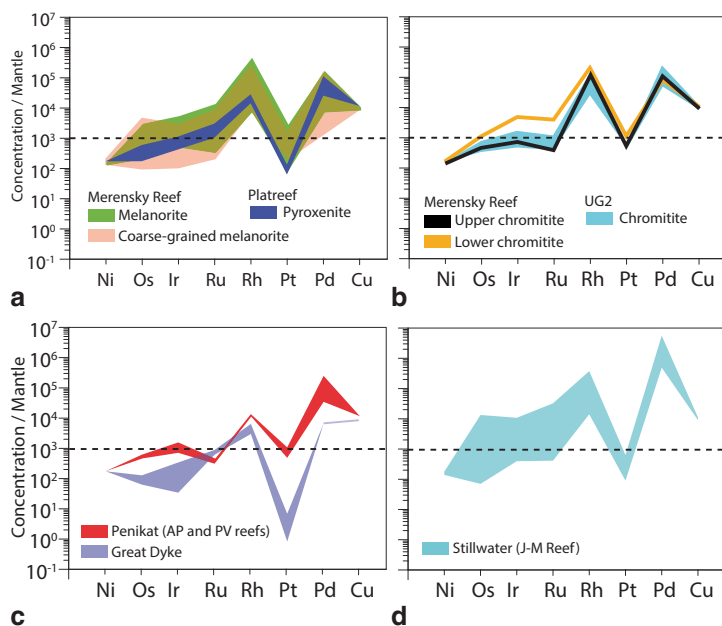


**Fig. 9.17** Mantle-normalized base-metal and platinum-group element spectras of pentlandite analysed from various PGE deposits. **a** Pentlandite from the Merensky Reef coarse-grained melanorite and melanorite (Godel et al. 2007; Osbahr et al. 2013) and pentlandite from the Platreef pyroxenite (Holwell and McDonald 2007) **b** Pentlandite from the Lower and Upper chromitite layers from the Merensky Reef (Godel et al. 2007) and the UG2 chromitite (Osbahr 2012). **c** Pentlandite from the Ap and PV Reefs of the Penikat intrusion and from the Main Sulfide Zone of the Great Dyke (Barnes et al. 2008). **d** Pentlandite from the JM Reef of the Stillwater Complex (Godel and Barnes 2008b)

and McDonald 2007; Holwell et al. 2006; Locmelis et al. 2010; Oberthür et al. 2003; Osbahr 2012; Osbahr et al. 2013; Rudashevsky et al. 2009; Rudashevsky et al. 2004; van der Merwe et al. 2012; Yudovskaya et al. 2012). These studies complemented the extensive literature available (e.g. Alapieti and Lahtinen 1986; Cawthorn et al. 2002; Kingston and El-Dosuky 1982; Kinloch 1982; Kinloch and Peyerl 1990; Lee 1996; McLaren and De Villiers 1982; Prichard et al. 2004). A wide range of PGM has been reported in various deposits and localities around the world (see Cabri (2002) and references therein for details) and included notably PGE-rich sulfides, tellurides and bismuthotellurides, arsenides, antimonides or alloys. Overall, the PGM assemblages and their textural relationships with other phases vary from one deposit to the other and might vary from one location to the other within the same deposit (Figs. 9.21 and 9.22). It is out of the scope of the present contribution to discuss all the details of PGM mineralogy in various deposits. The PGM are predominantly, if not exclusively, formed at low temperatures after the PGE have reached their present sites of accumulation within homogeneous droplets of sulfide liquid. Hence their identities are of secondary importance in the discussion of petrogenesis of PGE mineralization. For further information the reader is invited to consult the references given.



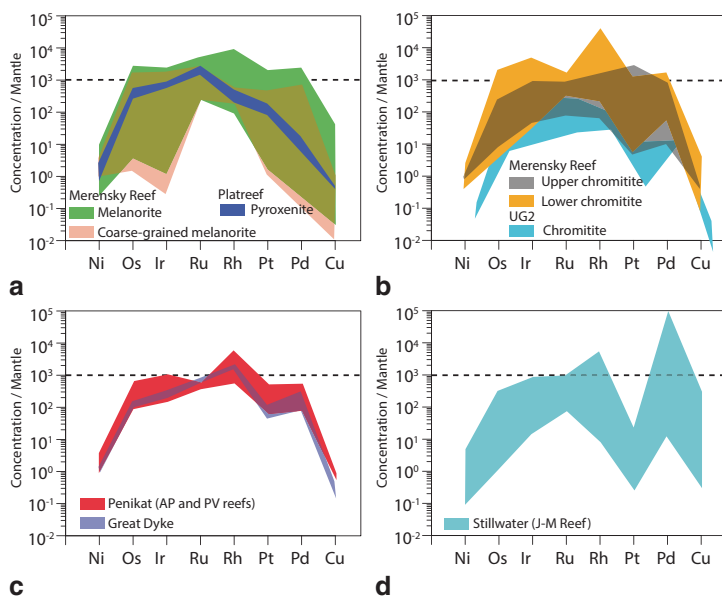


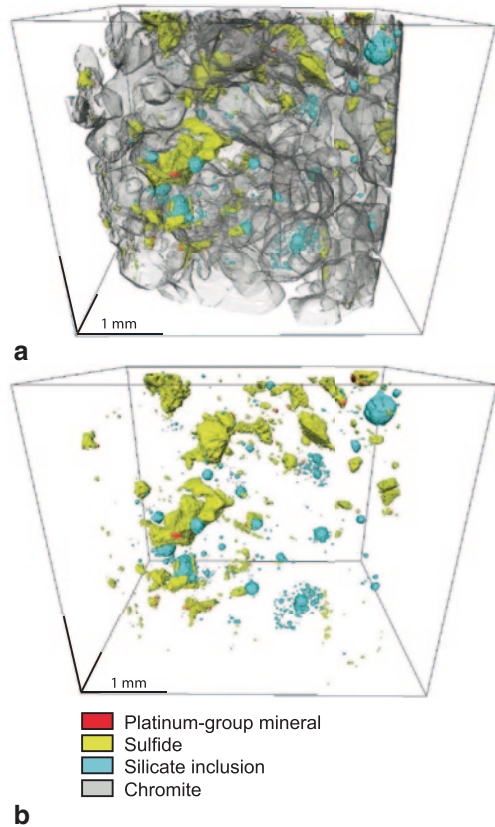
**Fig. 9.18** Mantle-normalized base-metal and platinum-group element spectras of pyrrhotite analysed from various PGE deposits. **a** Pyrrhotite from the Merensky Reef coarse-grained melanorite and melanorite (Godel et al. 2007; Osbahr et al. 2013) and pyrrhotite from the Platreef pyroxenite (Holwell and McDonald 2007). **b** Pyrrhotite from the Lower and Upper chromitite layers from the Merensky Reef (Godel et al. 2007) and the UG2 chromitite (Osbahr 2012). **c** Pyrrhotite from the AP and PV Reefs of the Penikat intrusion and from the Main Sulfide Zone of the Great Dyke (Barnes et al. 2008). **d** Pyrrhotite from the JM Reef of the Stillwater Complex (Godel and Barnes 2008b)

## Ore Forming Processes

The formation of PGE ore deposits requires that the PGE be concentrated about three to four orders of magnitude relative to Earth's mantle and crust concentrations, and two to three orders of magnitude over concentrations in inferred parent magmas to reef-bearing intrusions. This is a similar degree of concentration to that involved in other magmatic ore layers such as chromite seams and vanadiferous magnetite layers.

The PGE concentrations within a given orebody are influenced by a combination of processes that may occur at various stages of its history during: (i) mantle melting; (ii) the magma ascent and its emplacement into the crust; (iii) the crystallization of the magma to form a layered intrusion and; (iv) late to post-magmatic events such as hydrothermal alteration and metamorphism. One of the main challenges is the evaluation of the influence of each of the above factors in the control of ore genesis. In most of the deposits, the processes are complex with superimposition of physical and geochemical processes over a large range of temperature. The main factors that have been considered as controlling the genesis of PGE deposits in layered intrusion are reviewed and discussed below.

**Fig. 9.19** 3D distribution of chromite, base-metal sulfides, platinum group mineral and silicates inclusions in a sample of Lower Chromitite layer from the Merensky Reef. The 3D distribution of the minerals has been determined using high-resolution x-ray computed tomography and dedicated image analysis workflow. In most cases, the platinum-group minerals are located at the triple junction between sulfide, chromite and silicate minerals. A detailed description of the platinum-group minerals textural relationship with sulfides and chromite is provided in Godel et al. (2010). The origin of the different chromite morphologies and silicate inclusions are discussed in Vukmanovic et al. (2013)



## *Mantle Processes and Parental Magmas*

### **Platinum-Group Elements in the Earth's Mantle**

Platinum-group elements concentrations in the Earth's primitive mantle vary from ~1 to 7 ppb (McDonough and Sun 1995). The PGE are typically hosted by micron-scale base-metal sulfides and alloys that represent an extremely minor volume proportion (typically less than 0.1%) of the mantle (Lorand et al. 2008b). Detailed mineralogical investigation coupled with in situ mineral geochemistry of peridotite samples provided information on the residency of PGE in the lithospheric mantle (Alard et al. 2000; Lorand and Alard 2001; Lorand et al. 2008a; Lorand et al. 2008b; Luguet et al. 2007). These studies have revealed that more than 90% of the PGE in mantle lherzolites are hosted by base-metal sulfides. Alard et al. (2000) identified two different populations of sulfides: (i) Fe–Ni monosulfide solid solution (mss) observed as inclusions within olivine and (ii) Fe–Ni sulfide (pentlandite) and Cu–Fe sulfides (chalcopyrite and cubanite) observed at olivine contact boundaries.

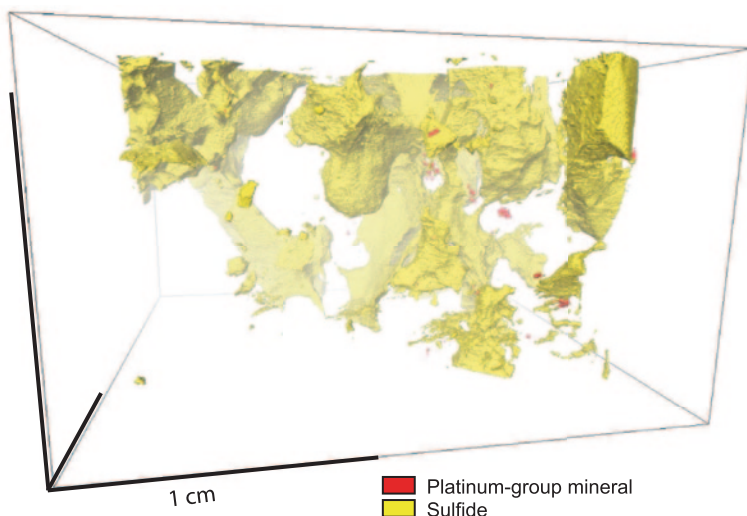


**Fig. 9.20** 3D distribution of base-metal sulfides and platinum-group minerals in a sample of olivine cumulate from the JM Reef Stillwater. In 3D, the platinum-group minerals are observed either at the contact between base-metal sulfides and silicates or in most cases in alteration haloes around the base-metal sulfides. In that cases, the platinum-group minerals are not touching the sulfide boundaries

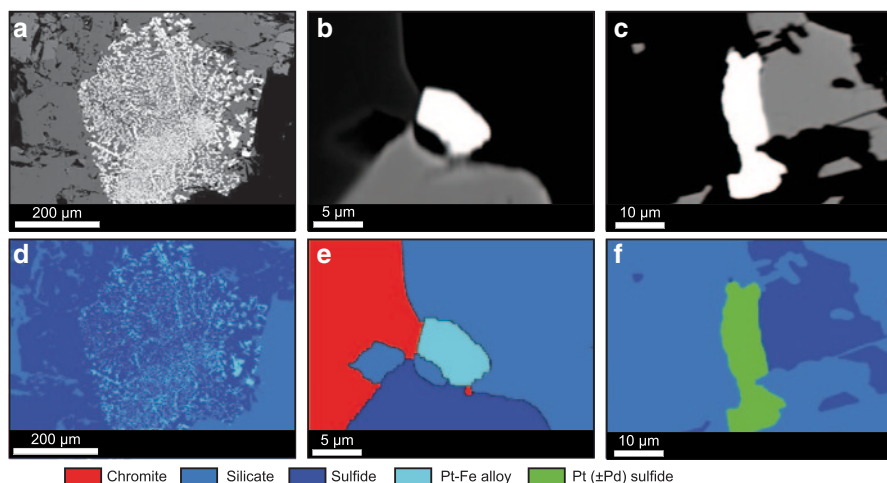


**Fig. 9.21** Examples of platinum-group minerals observed within the Merensky Reef, Rustenburg Platinum Mine (Bushveld Complex). **a** Backscattered electron and analysed **d** images showing symplectites of Pt-Fe alloy and base-metal sulfide minerals (pyrrhotite) at the contact with orthopyroxene (silicate). The image is modified from Godel et al. (2007). **b** Backscattered electron and analysed **e** images of euhedral Pt-Fe alloy in contact with chromite, sulfide and silicate. **c** Backscattered electron and analysed **f** images of Pt( $\pm$ Pd) sulfide located at the contact between sulfide and silicate

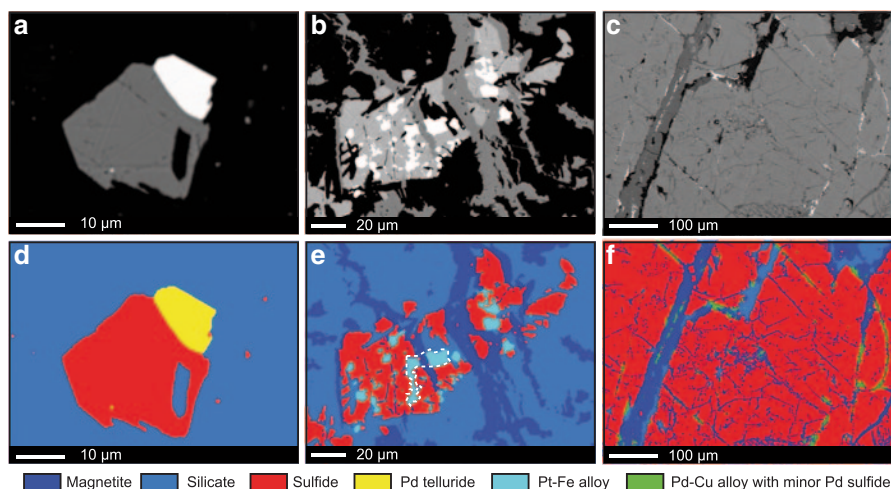


**Fig. 9.22** Examples of platinum-group minerals observed within the JM Reef, East Boulder Mine (Stillwater Complex). **a** Backscattered electron and analysed **d** images showing the association between Pd telluride, base metal sulfides and silicates. **b** Backscattered electron and analysed **e** images showing the complex associated between base-metal sulfide, Pt–Fe alloy and secondary magnetite. The primary Pt–Fe alloy and base-metal sulfides are crosscut by secondary magnetite (e.g. white tie line on **e**). The figure is modified after Godel and Barnes (2007). **c** Backscattered electron and analysed **f** images showing the complex association between base-metal sulfides, secondary magnetite and Pd–Cu alloy and minor Pd sulfides. In this sample, the Pd–Cu alloy is observed crosscutting the base metal sulfide over a distance of several millimetres and is also observed associated with the secondary magnetite,

Osmium, Ir, Ru and Rh were concentrated in the Fe–Ni mss whereas Pd and to a lesser extent Pt was enriched in the interstitial sulfides. The particular textural characteristics, mineralogy and geochemistry of these sulfides influences the composition of melts derived from lithospheric mantle as presented below. However, no information is available on the PGE residency in asthenospheric mantle sources, such as mantle plumes, that are widely regarded as the likely sources of magmas for large intracratonic layered intrusions (Arndt 2013), notwithstanding arguments for a dominantly lithospheric source for Bushveld magmas (Richardson and Shirey 2008). The argument about the nature and PGE content of mantle sources is likely to continue.

### Platinum-Group Elements Behaviour During Partial Melting of the Mantle

Partition coefficients of PGE between sulfide and silicate melts are in the order of  $10^4$ – $10^5$  (Barnes and Lightfoot 2005 and references therein), and possibly much higher (Fonseca et al. 2009, Mungall and Brenan, 2014). Hence, at equilibrium the concentration of a given PGE in a sulfide melt is typically at least four orders of magnitude larger than in coexisting silicate melt. Hence, the igneous geochemistry

of sulfur, and in particular the mass balance of equilibrating silicate and sulfide liquid (Campbell et al. 1983) strongly controls the behaviour of the PGE. Primary mantle-derived magmas show PGE concentrations ranging from 0.2 to ~40 ppb (Crocket 2002) with concentrations mainly depending on the behaviour of base-metal sulfides during partial melting of the mantle (Barnes et al. 1985) and subsequent sulfide liquid saturation history of the silicate magma. The solubility of sulfur in mantle-derived melts mainly depends on pressure (i.e. depth) and temperature of melting (Mavrogenes and O'Neill 1999). Sulfur solubility in typical basalts broadly ranges from 500 to 1000 ppm with sulfur solubility of ~800 ppm at temperature of 1400 °C and a depth of 120 km. Low to moderate degrees of partial melting of typical mantle, thought to contain about 200–250 ppm sulfur, cannot lead to the entire dissolution of the sulfides (Barnes et al. 1985; Hamlyn and Keays 1986). In that case, residual Fe–Ni sulfides sequestering some PGE remains in the mantle (Bockrath et al. 2004a). As a result, magma derived from low to moderate degrees of partial melting (i.e. <20%) of the mantle (e.g. mid-ocean ridge basalts) have low PGE concentrations and exhibit poor potential for forming subsequently economic PGE deposits. In contrast, at high degree of partial melting (generating komatiites or picritic continental flood basalts) all the sulfur present in the mantle is dissolved and all the PGE are transferred to the silicate melt. The PGE concentration in the silicate magmas are dictated by the partition coefficient of host mineral and melt and fractionation of Pt and Pd relative to Ir, Os, Ru and Rh may be observed (Mungall and Naldrett 2008). All of the major known PGE-deposits on Earth originated from high-degree of partial melting of the mantle and are related to intraplate picritic, or possibly komatiitic magmatism (Wilson 2012). However at high oxygen fugacity ( $f_{O_2}$ ), sulfides in the mantle may (partially or entirely) convert to sulfate leading to a strong increase in sulfur solubility in the melt (Jugo 2009; Jugo et al. 2005; Mungall 2002b; Mungall et al. 2006). In that case, even a small degree of partial melting may result in the consumption of all the sulfur present in the mantle (Dale et al. 2012). Hence, magmas formed under these oxidizing-conditions may have potential to generate economic PGE deposits, provided that the dissolved sulfur can subsequently be reduced to sulfide. In addition, several events of melting can occur and complicate the predictions of PGE behaviours in the magma. To date, little is known about the form of the PGE in the melt and whether they are completely dissolved or form nano-to micro particles enriched in Ir, Os and Ru that may be transported by the melt upon its ascent into upper crustal level (Bockrath et al. 2004a).

### **Fractionation of Platinum-Group Elements and Parental Magmas**

Fertile magmas form under sulfide-undersaturated conditions. Once a fertile silicate magma is formed it needs to ascend from the mantle to the upper level of the crust where it can potentially form a PGE deposit. During its ascent the magma becomes strongly undersaturated in sulfide (i.e. sulfide liquid are unlikely to form and collect PGE) as a result of decreasing pressure (Mavrogenes and O'Neill 1999; Wendlandt

1982). Fractionation (mostly resulting from the process of fractional crystallization of olivine) may potentially lead to a change in PGE concentrations. Experimental studies of the solubility and partitioning of PGE between olivine and silicate melt (Brenan et al. 2005; Brenan et al. 2003) suggested that olivine-silicate melt partition coefficients for Rh, Ru, and Ir increase with decreasing oxygen fugacity ( $fO_2$ ) to reach value of  $\sim 2$  at  $fO_2$  relevant to mafic and ultramafic igneous systems. In contrast, Pt and Pd behave incompatibly during olivine fractionation. The difference in behaviour between the IPGE (Ir, Os, Ru,) and the PPGE (Pt, Rh, Pd) during olivine fractionation may account for some of the observed variation in IPGE/PPGE ratios variation in primitive high MgO, sulfur poor magmas (Puchtel and Humayun 2000). Overall the solubility of IPGE in silicate melt is very low suggesting that IPGE-rich alloys may form and be included with olivine and chromite (Brenan et al. 2005a). The incorporation of IPGE-rich alloys in chromite was demonstrated experimentally and justified with thermodynamic models by Finnigan et al. (2008). That hypotheses was confirmed Barnes and Fiorentini (2008), based on the analysis of a large body of data on komatiites. Many other studies have also documented the occurrence of PGE alloys in mantle peridotite (Kogiso et al. 2008; Lorand et al. 2010; Luguét et al. 2007). Recent work by Park et al. (2013) suggested the existence of Pt alloy in some arc magma sources.

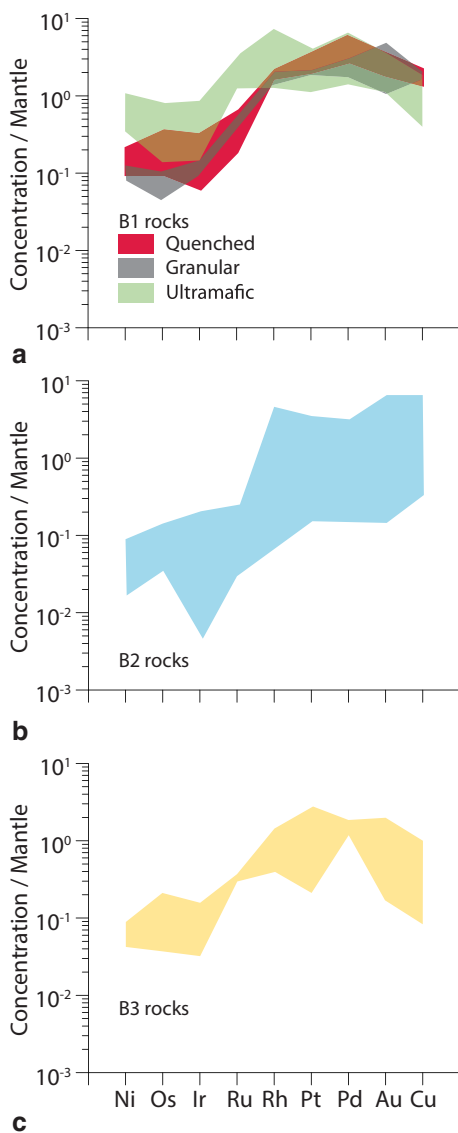
Proposed parental magmas to most of the layered intrusions hosting PGE-deposits (e.g. Bushveld Complex, Stillwater Complex, and Great Dyke) are in equilibrium with high-magnesian olivine ( $\sim Fo_{90}$ ) and probably represent primary magmas that have not been significantly affected by fractionation during their ascent (Cawthorn et al. 2005). Hence, their PGE concentrations may be similar to those present in primary magma. The estimation of parental magma of a layered intrusion is relatively difficult as several issues arise in the estimation of the parental magma from the chilled margins or the fine-crystallized rocks spatially associated with an intrusion as they may not necessarily be representative of the parental magma of the intrusion that they are associated with (Godel et al. 2011 and references therein). Current estimates of the composition of the Bushveld Complex parental magmas (Barnes et al. 2010 and reference therein) indicate that Pt and Pd concentrations vary from 10 to 25 ppm ppb and 3 to 15 ppb, respectively (Fig. 9.23). Recently, Mungall and Brenan (2014) demonstrated, based on new experiments and modelling, that this unremarkable PGE concentrations in the parental magmas are enough to explain the occurrence of high grade ore occurrences providing suitable conditions are reached.

### ***Role of Base-Metal Sulfide Liquids***

With the rare exception of some PGE-rich chromitites, most of the PGE deposits observed within layered intrusions presented above are associated with the presence of magmatic base- metal sulfides (typically forming intergrowths of pyrrhotite, pentlandite and chalcopyrite). These sulfides represent the accumulation of primary immiscible sulfide liquid that segregate from the silicate magma.



**Fig. 9.23** Estimate of platinum-group element concentrations in the inferred parental magmas of the Bushveld complex. The concentrations for various magma types are extracted from Barnes et al. (2010) and presented are mantle-normalized base-metal and PGE patterns. The normalization values are from McDonough and Sun (1995)



### Sulfur Solubility

The sulfur concentration in a silicate melt depends on parameters (total pressure, temperature, oxidation state and melt composition) that control the sulfur speciation and solution mechanisms (see detailed review in Mungall (2014) and Ariskin et al. (2013) for further information). The sulfur concentration at sulfide saturation (SCSS) depends mainly on the melt composition (particularly the Fe content), temperature, pressure and oxygen fugacity ( $fO_2$ ). In addition to Fe, chalcophile elements such as

Ni and Cu (Ariskin et al. 2009; Ariskin et al. 2013; Ariskin et al. 2010; Evans et al. 2008) and some of the PGE (Laurenz et al. 2013) may also play a significant control on sulfur solubility in ultramafic and mafic magmas. Over the past few years, empirical (Ariskin et al. 2009; Ariskin et al. 2010; Li and Ripley 2009; Li and Ripley 2005) and experimental (Liu et al. 2007) models have been developed to predict the sulfur concentration at sulfide saturation. Typical basaltic magmas can dissolve or contain ~800–1000 ppm sulfur and are typically sulfide undersaturated in the crust.

Sulfide saturation may be provoked by external factors such as magma cooling and crystallization, mixing of magma with different compositions and the assimilation of crustal rocks by the primitive magmas as described below.

### **PGE Collection by Sulfide Liquid**

During cooling and crystallization, sulfur is incompatible in the crystallising phases and hence, its concentration increases progressively as the magma fractionates. Ultimately, the sulfur concentration in the magma may reach the value at which immiscible sulfide liquid forms (i.e. SCSS described above). In the absence of external factors favouring sulfide saturation, a large degree of crystallization may be required before that sulfide liquid form. Hence, the sulfide liquid may segregate from highly evolved silicate magma with ferrobasalt composition (e.g. after ~60–70% crystallization at Skaergaard or Sonju Lake intrusions). In general, the sulfide saturation will occur after Ni has been depleted as a result of olivine crystallization (Jenner et al. 2010; Ripley and Li 2013). Platinum, Pd and Cu are incompatible in the silicate and oxides crystallizing and hence their concentrations in the magma increase (Wohlgenuth-Ueberwasser et al. 2013). Lowering of  $\text{Fe}^{2+}$  activity as a result of extensive magnetite crystallization may lead to sulfide saturation. In that case, the sulfide that form are Cu–Fe and potentially PGE-rich (e.g. bornite-chalcocite-skaergaardite assemblage in the Platinova Reef of the Skaergaard intrusion). At low degrees of supersaturation, the immiscible sulfide droplets that form are expected to be widely spaced and will grow by diffusion processes (Mungall and Su 2005). Once the droplets have grown past a certain diameter, they will sink toward the bottom of the magma chamber, a process similar to fractional crystallization of the silicate. The first immiscible sulfide to form will be highly enriched in the PGE with PGE concentrations depending mainly on their partition coefficients and their diffusion rate in growing sulfide droplets (Mungall 2002a). The variability in degree of supersaturation, diffusivity rates and to a lesser extent partition coefficients between different PGE may lead to an offset in sulfide abundance and concentrations of different PGE (Mungall 2002a; Mungall 2007) as observed for the Great Dyke (Wilson and Prendergast 2001) and the Munni Munni intrusion in Australia (Barnes 1993).

The most popular model of formation of PGE reef is a model whereby the PGE are collected by an immiscible sulfide liquid (Figs. 9.24a, b and c) that form as a result of magma recharge and mixing (Barnes and Maier 2002b; and Naldrett 1979a; Campbell et al. 1983; Godel et al. 2007; Maier and Barnes 1999; Mungall and Brenan 2014; Naldrett et al. 2009a). Li and Ripley (2009) tested that hypothesis and

showed that mixing of two different magmas may result in the attainment of sulfide saturation in the hybrid magma. An important prerequisite is that each magma should have sulfur concentration sufficiently high to be close to their concentration at sulfur saturation. Small to moderate degree of saturation in the hybrid magma will lead to the formation of a small amount of sulfide liquid. In contrast, assimilation of crustal sulfur by the magma may enhance the sulfur saturation process and lead to the formation of large amounts of sulfides and a potentially to the dilution of preexisting PGE-rich sulfide melt (e.g. the Platreef (Hutchinson and McDonald 2008; Sharman et al. 2013). In all cases, once sulfide droplets have formed they will interact with their surrounding environment in a manner that mainly depends on physical properties and constraint. In a layered intrusion, the newly formed droplets are expected to grow and settle and accumulate to the bottom of the magma chamber when their size is large enough to overcome gravity constraint. Under particular conditions (Chung and Mungall 2009; Mungall and Su 2005 and Chap. 8), the sulfide droplets may coalesce to form 3D networks of interstitial sulfide liquid that may percolate downwards into the crystallizing cumulus mineral pile until it reaches an area where no further migration is possible (Godel et al. 2006).

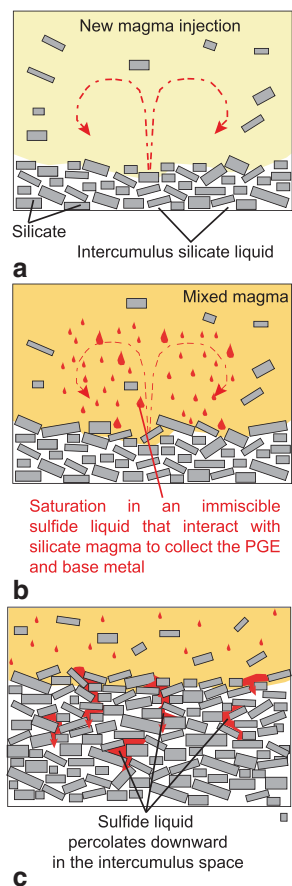
The base-metal and PGE concentrations in the sulfide liquid ( $C_{Sul}$ ) is mainly depending on the partition coefficient between sulfide and silicate melt and the bulk metal concentration and is best described, in a closed system, by Campbell and Naldrett (1979) equation:

$$C_{Sul} = C_0 D^{Sul/Sil} \frac{R+1}{R+D^{Sul/Sil}}$$

where  $C_0$  is the concentration of a given metal in the original silicate liquid,  $D^{Sul/Sil}$  is the partition coefficient (for each metal) between the sulfide and the silicate liquids, and  $R$  is the mass ratio of silicate to sulfide liquid. Hence, if small amounts of sulfide form in a magma chamber (i.e. high  $R$ -factor) their PGE concentration will be large, typically those found in PGE reef deposits (Campbell et al. 1983). In contrast, if the amount of sulfide that forms is significant relative to the host magma (i.e. low  $R$ -factor), the PGE concentration in the sulfide will be diluted and may not be sufficient to make economic PGE ore grades. However, if a large amount of sulfide is available, it may represent an interesting target for Ni and Cu deposit where PGE will be a byproduct. In rare case such as the Platreef, suitable parental magma combined with various amounts of assimilation of crustal sulfur may lead to the formation of an exceptional PGE-deposit (Sharman et al. 2013 and references therein).

The equation of Campbell and Naldrett (1979) has successfully and widely been applied to model metal concentrations observed in a variety of magmatic ore deposits (Naldrett 2004 and references therein). Notably, the application of this equation to the silicate rocks of the Merensky Reef (Barnes and Maier 2002b; Godel et al. 2007) indicates that the PGE present in solid-solution of the base-metal sulfide and observed as platinum-group minerals closely associated with the sulfide can be accommodated in a sulfide liquid. This sulfide liquid interacted with a large volume of magma with metal compositions similar to that suggested for the Bushveld

## PGE collection by sulfide liquid



## PGE collection by aqueous fluid

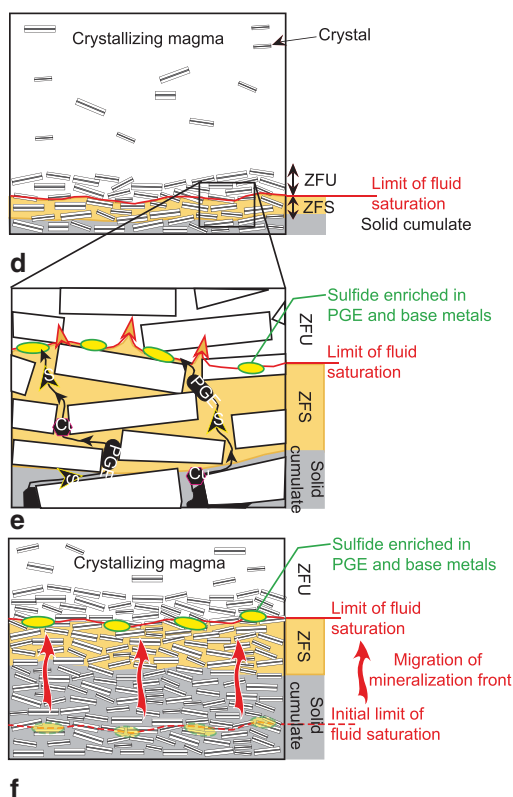


**Fig. 9.24** Schematic diagram illustrating proposed model of formation of platinum-group element deposits in silicate rocks (modified after Godel, 2007). **a**, **b** and **c** Model of PGE collection by an immiscible magmatic sulfide liquid that segregate from the magma and then percolate downwards in the interstices between cumulus minerals. See text for further explanation and reference. **d**, **e**, and **f** Model of PGE collection by an aqueous fluid that percolates upwards into the cumulate pile as it crystallises. ZFU zone of fluid undersaturation, ZFS zone of fluid saturation. See text for further explanation and reference

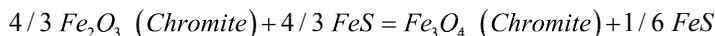
Complex (Barnes et al. 2010). During cooling, the PGE and Pt in particular may exsolve from the sulfide as platinum-group minerals or in some case partition into a semi-metal and sulfarsenide melt that subsequently crystallize as platinum-group minerals (Fig. 9.25). This combination of processes accounts for the range of geochemical and textural features observed in the silicate rocks of the Merensky Reef.

In contrast, the PGE (mainly Pt, Ir, Os and Ru) concentrations observed in PGE-rich (often sulfide poor) chromitite layers of the Merensky Reef (Barnes and

Maier 2002b; Godel et al. 2007) and large PGE-rich chromitite layers (Maier and Barnes 2008; Naldrett et al. 2011b; Naldrett 2004) are too high to be solely explained by a process of PGE collection by an immiscible sulfide liquid, unless partition coefficients are at the extreme limit of the range that has been determined on experimental evidence (Fonseca et al. 2009), and R-factor values are at the upper limit of plausibility. Cawthorn et al. (2005) have argued that this combination of circumstances is unlikely, although Kerr and Leitch (2005) have proposed a mechanism of multi-stage dissolution and re-enrichment of sulfide liquid that could account for extreme PGE enrichment. Application of this model to the Merensky Reef was presented in Godel et al. (2008a) and Naldrett et al. (2012).

### ***PGE-Enrichment in Chromitite Layers***

Several processes have been proposed to explain the particular PGE enrichment and metal ratios observed in chromitite layers and the predominance of platinum-group minerals on the PGE-budget. Naldrett and Lehmann (1988) suggested that primary PGE-rich magmatic sulfide trapped within the chromitite could react with chromite to produce a Fe-rich chromite and remove sulfur from the system according to the reaction:



Consequently, this reaction lowers the sulfur fugacity ( $fS_2$ ) and could have resulted in the partial desulfurization of the sulfide leading to the formation of residual monosulfide solid solution, Fe–Pt alloys and Cu–Pd rich sulfide melt (Peregoedova et al. 2004). This model can explain the fact that the sulfides in the chromitite layers of the Bushveld Complex exhibit high PGE/ sulfur ratios and are generally enriched in Cu and to a lesser extent Ni. By considering this hypothesis, the chromitite layers should have originally contained at five to ten times more sulfides than they do now and all the PGE were originally hosted in the sulfide liquid. The model does not explain the reason why the chromitite layers exhibit Pd concentrations lower than those of the other PGE. Two other possibilities have been envisaged to explain the particular features observed in chromitite layers and are related to the early formation of platinum-group minerals. Evidence of the direct crystallization of laurite ( $\text{RuS}_2$ ) from a sulfide-undersaturated silicate melt has been provided experimentally and thermodynamically (Andrews and Brenan 2002; Bockrath et al. 2004b; Brenan and Andrews 2001). Based on PGE mass balance and geochemical modelling in the Merensky Reef chromitites, Barnes and Maier (2002b) and Godel et al. (2007) proposed that some of the PGE may crystallise as platinum-group minerals (mainly laurite and Pt alloy) before an immiscible sulfide liquid forms, and these PGMs are collected by crystallizing chromite. Subsequent, sulfide liquid formation collected the remaining PGE. Finnigan et al. (2008) carried out experiments involving the growth and reequilibration of chromite crystals in a silicate melt. In these experiments, platinum-group minerals (mainly laurite and IPGE alloys) formed at the in-

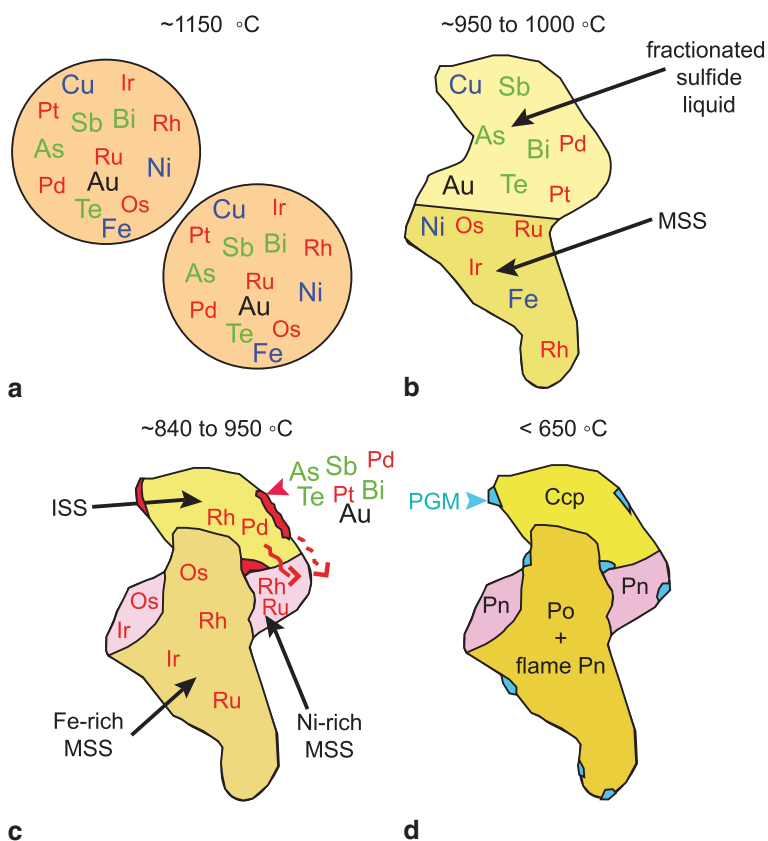


**Fig. 9.25** Schematic diagram summarizing the behaviour of platinum-group elements, base metal and other chalcophile elements during the formation of a base metal sulfide liquid and its cooling (modified after Barnes et al. 2006). **a** Immiscible sulfide liquid droplets form and collect the PGE and other chalcophile elements. **b** On cooling, the sulfide liquid fractionates leading to the formation of monosulfide solid solution (*MSS*) and fractionated Cu-rich sulfide liquid. **c** Further cooling lead to the crystallization of intermediate sulfide solid-solution (*ISS*) and Ni-rich *MSS* from the fractionated sulfide liquid. In some cases, sulfosalt melts (i.e. As, Sb, Te or Bi bearing) may formed and collect some of the PGE. These melts may migrate along sulfide/silicate boundaries. **d** At temperature <At tC, pyrrhotite and pentlandite exsolve to form the *MSS* and chalcopyrite from the *ISS* and platinum-group minerals crystallized from the sulfosalt melt

interface between the chromite crystal and the silicate melt. Based on their results, the authors proposed that the platinum-group minerals may precipitate as a result of local reduction around chromite crystal, probably caused by the preferential uptake of  $\text{Fe}^{3+}$  and  $\text{Cr}^{3+}$  by the chromite crystal relative to the melt. During the crystallization of the chromite, the local reduction triggers a decrease (by few percent) of the metal solubility at the crystal/melt interface leading to the formation of the platinum-group minerals that are subsequently trapped by the growing chromite. To date no consensus exists on the origin of PGE enrichment in chromitite layers and it remains a controversial topic. An alternative model was proposed by Latypov et al. (2013 and

references therein) to explain the lithological and textural relationships observed. In this model, the chromitites are interpreted to have formed by *in situ* growth directly at a crystal–liquid interface and the PGE are scavenged by sulfide droplets from fresh magma continuously brought towards the base by convection. The convection allows the sulfide to equilibrate with picritic magma of thousands to million times their own volume, resulting in sulfide high PGE tenor.

### ***Role of Fluids on PGE Distribution and Redistribution***

Experimental studies have shown that the base metals and the PGE may be transported by fluids of various compositions and within a large range of temperature (Baker et al. 2001; Hanley et al. 2005; Peregoedova et al. 2006; Wood 2002 and references therein). Details of the geochemistry of the PGE in low-to high temperature hydrothermal and magmatic fluids are presented in Hanley (2005) and a recent review by Barnes and Liu (2012). Evidence of PGE transport and reprecipitation has been observed at various scales and in different geological settings (Augé et al. 2005; Bursztyn and Olivo 2010; Cabral et al. 2002; El-Ghorfi et al. 2006; Molnar et al. 2001; Moroni et al. 2001; Olivo et al. 2001).

### **Platinum-Group Elements Collection by Deuteric Fluids**

The common observation of pegmatoidal textures, the presence of fluid and hydrous melt inclusions and the presence of Cl-rich apatites (i.e. having high Cl/F ratios) associated with PGE mineralization has led some authors to propose that the PGE-rich horizons observed in layered intrusions resulted from the percolation of Cl-rich aqueous fluid that carried and redeposited the PGE (e.g. Ballhaus and Stumpf 1986; Boudreau 2008; Boudreau and McCallum 1986; Boudreau and Mc Callum 1992a, b; Kanitpanyacharoen and Boudreau 2013; Vermaak and Hendriks 1976; Von Gruenewaldt 1979; Willmore et al. 2000). In this type of model (Figs. 9.24d, e and f), H<sub>2</sub>O dissolved in silicate magmas and intercumulus fractionated silicate liquid becomes progressively saturated in aqueous Cl-rich fluid as the crystal pile solidifies. The Cl-rich aqueous fluid collects the base-metals and the PGE as it migrates upward through the compacting cumulate pile. The base-metal and PGE are transported in solution until it reaches the interface where the intercumulus silicate liquid is not saturated in Cl-rich aqueous fluid. At this interface, the fluid dissolves in the intercumulus silicate liquid and PGE-rich base-metal sulfides with a mineralization front moving upwards as the limit of fluid saturation in the intercumulus silicate liquid migrates, ultimately forming a base-metal and PGE-rich sulfide horizon (Boudreau 1999; Boudreau and Mc Callum 1992b). However, the application of this model to explain the entire complexity of the PGE-reefs remains controversial (Barnes and Maier 2002b; Cawthorn et al. 2005; Godel et al. 2007; Keays et al. 2012; Maier et al. 2013; Naldrett et al. 2009b; Osbahr 2012). The main arguments against this model are from the literature:



- (i) No anomalously-poor PGE concentrations or PGE-depletion are observed in the rocks below the mineralized horizons of the Bushveld Complex (Barnes and Maier 2002a; Barnes and Maier 2002b; Naldrett et al. 2009b) and the Stillwater Complex (Keays et al. 2012);
- (ii) PGE-reefs, in most of the cases, can be traced over large distances (100's km in the Bushveld Complex) and directly over a magmatic unconformity. Upward migration of fluids would lead to discordant features that are not related to magmatic stratigraphy.
- (iii) Iridium and Ru are considered to be insoluble in aqueous hydrothermal/magmatic fluids, hence it is difficult to reconcile this with the concentration observed in the reefs;
- (iv) In the Bushveld Complex, the mantle-normalized base-metal and PGE patterns of the mineralized horizons (e.g. Merensky Reef, Fig. 9.10) show shapes identical to those of the B1 magma (Fig. 9.23), suggesting that the same process concentrated all the PGE at the level of the reef (Fonseca et al. 2009).
- (v) The osmium isotopic composition of Bushveld Complex cumulates shows a sharp change towards more radiogenic compositions at the level of the Merensky reef (McCandless and Ruiz 1991). The Merensky Reef is as much a concentration of Os as it is of Pt and Pd, but the isotopic data imply that Os cannot have been derived from the underlying cumulates. In addition, there are places in the Bushveld Complex (e.g. the far southern limit of the eastern lobe) where the UG2 reef package sits on top of the footwall metasediments without underlying Rustenburg Layered Suite stratigraphy. Hence a model involving upward transport by fluids would require that concentrations of different PGEs occurred in the same rock by entirely different processes (Li and Ripley 2006; Li et al. 2004).

### Hydrothermal Remobilization of the Platinum-Group Elements

Evidences of post-cumulus remobilization of PGE in PGE reefs hosted within layered intrusion have notably been described for the JM-Reef of the Stillwater Complex (Godel and Barnes 2008a; Godel and Barnes 2008b), the Platreef (Holwell and McDonald 2006; Hutchinson and Kinnaird 2005; Yudovskaya et al. 2012). In the JM-Reef of the Stillwater Complex, detailed mineralogical analysis (Godel and Barnes 2008a; Godel and Barnes 2008b) of altered samples revealed the presence of Pd-Cu alloys (with composition similar to Skaergaardite (Rudashevsky et al. 2004)) and to a lesser extent Pd sulfides observed either as interstitial phase between magnetite crystal or as small veinlets crosscutting the base-metal sulfide minerals (Fig. 9.22). This observation suggests that Pd was mobile after the base-metal sulfides solidified and possibly added to the system during alteration or metamorphic processes that lead to the oxidation of the base-metal sulfides to magnetite. The origin, the scale and the extent of the Pd remobilization remain poorly constrained.

## Weathering and Remobilization of the Platinum-Group Elements

In the Main Sulfide Zone of the Great Dyke, primary magmatic PGE-rich sulfides have been oxidized during near-surface weathering and represent a challenge for geometallurgy (Locmelis et al. 2010; Oberthür and Melcher 2005). In this oxidized ore, the proportion of PGE found in solid solution of the base-metal sulfides is negligible but Pd concentration in relict pentlandite can reach 6500 ppm. Most of the Pt and Pd are hosted by relicts of primary and secondary platinum-group minerals. PGE released during the oxidation of the primary are redistributed and incorporated into Fe/Mn oxides/hydroxides and clay minerals leading to considerable local variation in the distribution of PGE.

The examples described above highlight the importance of considering hydrothermal processes over a range of temperatures (from low-temperature hydrothermal to high-temperature magmatic or hydrothermal) in the generation or modification of high grade PGE-ores.

## Conclusions

Over the past 10 years, technological developments (e.g. LA-ICP-MS, high-resolution X-ray computed tomography, isotope-ratio mass spectrometers) have allowed the acquisition of multidisciplinary dataset at spatial resolution, detection limits and precisions that were impossible to achieve in the past, in both 2D and 3D. The results obtained provided additional insights into the complexity of the ores, the residency of PGE in the rocks and the variability within and between different ore deposits and highlighted the necessity of adapting (for each deposit) models of formation based on all of the information available. Each PGE deposit is different and the processes that form them are complex. Models of formation may range from the primary accumulation of immiscible base-metal sulfide liquid to the late-stage (post-cumulus alteration or metamorphism) remobilization of the PGE and base-metal sulfides. It is clear that any model of formation of PGE-reefs needs to consider the superimposition of both physical and geochemical processes, over a range of scale and over a wide range of temperature (Fig. 9.26) to successfully account for the observed petrographic and mineralogical complexities.

**Acknowledgments** James Mungall, Ian McDonald and Rais Latypov (associate editor) are thanked for their comments and suggestion that improve the quality of the manuscript. Steve Barnes, Patrick Nadoll and Ludovic Ricard are acknowledged for their suggestions during CSIRO internal review processes. This is a contribution from the CSIRO Mineral Down Under Flagship.

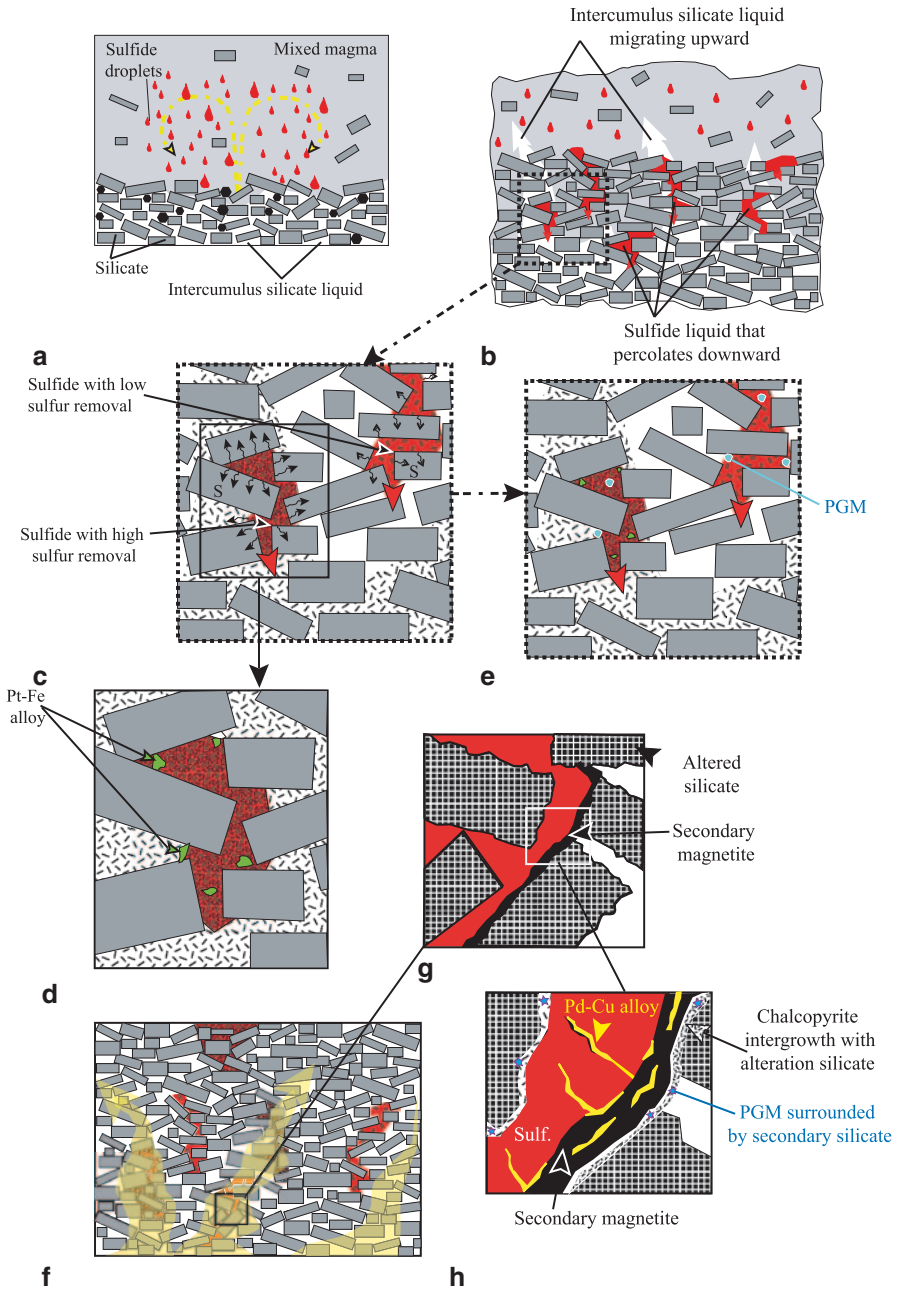


**Fig. 9.26** Schematic diagram summarizing the processes that might be involved in the formation and modification of PGE-reef type deposits. **a** Immiscible magmatic sulfides form as a result of magma mixing, crustal contamination and/or crystal fractionation. **b** The sulfide droplets collect the base metal and PGE, settle in the magma chamber and potentially accumulate and coalesce while percolating downward into the cumulus mineral framework. **c** Intercumulus silicate melts or

## References

- Alapieti TT, Halkoaho TAA (1995) Cryptic variation of augite in the Penikat Layered Intrusion, Northern Finland, with reference to megacyclic units and PGE-enriched zones. *Mineral Petrol* 54(1–2):11–24
- Alapieti TT, Lahtinen JJ (1986) Stratigraphy, petrology, and platinum-group element mineralization of the early Proterozoic Penikat layered intrusion, northern Finland. *Econ Geol* 81(5):1126–1136
- Alapieti TT, Lahtinen JJ (2002) Platinum-group element mineralization in layered intrusions of Northern Finland and the Kola Peninsula, Russia. In: Cabri LJ (ed) *Geology, Geochemistry, Mineralogy and Mineral beneficiation of Platinum Group Element*, vol Special Volume 54. pp 507–546
- Alard O, Griffin WL, Lorand JP, Jackson SE, O'Reilly SY (2000) Non-chondritic distribution of the highly siderophile elements in mantle sulfides. *Nature* 407(6806):891–894
- Andersen JCO, Rasmussen H, Nielsen TFD, Ronsbo JG (1998) The Triple Group and the Platinova gold and palladium reefs in the Skaergaard Intrusion—stratigraphic and petrographic relations. *Econ Geol* 93:488–509
- Andrews DRA, Brenan JM (2002) The solubility of ruthenium in sulfide liquid: implications for platinum group mineral stability and sulfide melt-silicate melt partitioning. *Chem Geol* 192:163–181
- Ariskin AA, Barmina G, Bychkov K, Danyushevsky L (2009) Parental magmas of mafic layered intrusions: using an updated COMAGMAT model for calculations of sulfide-silicate cotectics during their crystallization. In: *Proceedings of Xi-an International Ni–Cu(Pt) Deposit Symposium 2009*, vol., Xi'an
- Ariskin AA, Danyushevsky LV, Bychkov K, Barmina GS (2010) Modeling sulfide solubility in MORB glasses and olivine cumulate piles: the opposite effect of NiO versus FeO in the melt. In: Survey OG (ed) *11th International Platinum Symposium*, vol Abstract volume, Miscellaneous Release. Sudbury, Ontario, Canada, pp 1–4
- Ariskin AA, Danyushevsky L, Bychkov KA, McNeill AW, Barmina G, Nikolaev GS (2013) Modelling solubility of Fe–Ni sulfides in basaltic magmas: the effect of Ni. *Econ Geol* 108(8):1983–2003
- Arndt NT (2013) The lithospheric mantle plays no active role in the formation of magmatic ore deposits. *Econ Geol* 108(8):1953–1970
- Arndt NT, Leshner CM, Czamanske GK (2005) Mantle derived magmas and magmatic Ni–Cu–PGE deposits. *Econ Geol* 100th Anniversary Volume:5–24
- Augé T, Petrunov R, Bailly L (2005) On the origin of the PGE mineralization in the elatsite porphyry Cu–Au deposit, Bulgaria: comparison with the Baula-Nuasahi complex, India, and other alkaline PGE-rich porphyries. *Can Mineral* 43:1355–1372
- Baker DR, Barnes S-J, Simon G, Bernier F (2001) Fluid transport of sulfur and metals between sulfide melt and basaltic melt. *Can Mineral* 39:537–546

---

magmatic fluids may percolate upward into the cumulate pile and potentially react with the base metal sulfide leading to area of localized desulfurisation **d** and the exsolution of some platinum-group minerals (e.g. Pt–Fe alloy). **e** On cooling, additional platinum-group minerals crystallise from the sulfides or from semi-metal or sulfosalt melts. The platinum-group minerals tend to form at the contact at the interface with the base-metal sulfides. **f** Post-cumulus hydrothermal or metamorphic events may lead to the remobilisation of PGE and to the crystallization of secondary PGM. In the example of the Stillwater Complex **g**, secondary magnetite is the host of secondary Pd–Cu alloy **h**. In addition, the base-metal sulfide may partially be replaced by secondary silicate. Insoluble platinum-group minerals are not affected and are observed as inclusion within secondary silicate without any visible textural relationship with sulfides

- Ballhaus CG, Stumpfl EF (1986) Sulfide and platinum mineralization in the Merensky Reef: evidence from hydrous silicates and fluid inclusions. *Contrib Mineral Petrol* 94(2):193–204
- Ballhaus C, Sylvester P (2000) Noble metal enrichment processes in the Merensky Reef, Bushveld Complex. *J Petrol* 41(4):545–561
- Barnes SJ (1993) Partitioning of the platinum group elements and gold between silicate and sulfide magmas in the Munni-Munni Complex, Western-Australia. *Geochim Cosmochim Acta* 57(6):1277–1290
- Barnes SJ, Fiorentini ML (2008) Iridium, ruthenium and rhodium in komatiites: Evidence for iridium alloy saturation. *Chem Geol* 257(1–2):44–58
- Barnes S-J, Lightfoot PC (2005) Formation of magmatic nickel sulfide deposits and processes affecting their copper and platinum-group element contents. *Econ Geol* 100th Anniversary Volume:179–213
- Barnes SJ, Liu W (2012) Pt and Pd mobility in hydrothermal fluids: Evidence from komatiites and from thermodynamic modelling. *Ore Geol Rev* 44:49–58
- Barnes S-J, Maier WD (2002a) Platinum-group element distributions in the Rustenburg Layered Suite of the Bushveld Complex, South Africa. In: Cabri LJ (ed) *Geology, Geochemistry, Mineralogy and Mineral beneficiation of Platinum Group Element*, vol Special Volume 54. Canadian Institute of Mining, Metallurgy and Petroleum, pp 553–580
- Barnes S-J, Maier WD (2002b) Platinum-group elements and microstructures of Normal Merensky Reef from Impala Platinum Mines, Bushveld Complex. *J Petrol* 43(1):103–128
- Barnes SJ, Naldrett AJ (1986) Geochemistry of the J-M Reef of the Stillwater Complex, Minneapolis adit area II. Silicate mineral chemistry and petrogenesis. *J Petrol* 27(4):791–825
- Barnes S-J, Naldrett AJ, Gorton MP (1985) The origin of the fractionation of platinum-group elements in terrestrial magmas. *Chem Geol* 53(3–4):303–323
- Barnes S-J, Cox R, Zientek M (2006) Platinum-group element, Gold, Silver and Base Metal distribution in compositionally zoned sulfide droplets from the Medvezky Creek Mine, Noril'sk, Russia. *Contrib Mineral Petrol* 152(2):187–200
- Barnes S-J, Prichard HM, Cox RA, Fisher PC, Godel B (2008) The location of the highly siderophile elements in platinum-group element rich ore deposits (a textural, whole rock geochemical and microbeam study): Implication for the formation of the deposits. *Chem Geol* 248:295–317
- Barnes S-J, Savard D, Bédard LP, Maier W (2009) Selenium and sulfur concentrations in the Bushveld Complex of South Africa and implications for formation of the platinum-group element deposits. *Miner Deposita* 44(6):647–663
- Barnes S-J, Maier WD, Curl EA (2010) Composition of the marginal rocks and sills of the Rustenburg Layered Suite, Bushveld Complex, South Africa: implications for the formation of the Platinum-Group Element Deposits. *Econ Geol* 105(8):1491–1511
- Barnes SJ, Osborne G, Cook D, Barnes L, Maier WD, Godel B (2011) The Santa Rita nickel sulfide deposit in the Fazenda Mirabela Intrusion, Bahia, Brazil: geology, sulfide geochemistry and genesis. *Econ Geol* 106:1083–1110
- Bird DK, Brooks CK, Gannicott RA, Turner PA (1991) A gold-bearing horizon in the Skaergaard Intrusion. *Econ Geol* 86(5):1083–1092
- Bockrath C, Ballhaus C, Holzheid A (2004a) Fractionation of the platinum-group elements during mantle melting. *Sciences* 305:1951
- Bockrath C, Ballhaus C, Holzheid A (2004b) Stabilities of laurite RuS<sub>2</sub> and monosulfide liquid solution at magmatic temperature. *Chem Geol* 208(1–4):265–271
- Boudreau A (1999) Fluid fluxing of cumulates: The J-M reef and associated rocks of the Stillwater complex, Montana. *J Petrol* 40(5):755–772
- Boudreau A (2008) Modeling the Merensky Reef, Bushveld Complex, Republic of South Africa. *Contrib Mineral Petrol* 158:431–437
- Boudreau A, McCallum IS (1986) Investigations of the Stillwater Complex: III. The Picket Pin Pt/Pd deposit. *Econ Geol* 81:1953–1975
- Boudreau AE, Mc Callum IS (1992a) Concentration of platinum-group elements by magmatic fluids in layered intrusions. *Econ Geol* 87(7):1830–1848

- Boudreau AE, Mc Callum IS (1992b) Infiltration metasomatism in layered intrusions—an example from the Stillwater Complex, Montana. *J Volcanol Geotherm Res* 52(1–3):171–183
- Brenan JM, Andrews DRA (2001) High-temperature stability of laurite and Ru–Ir–Os alloy and their role on PGE fractionation in mafic magmas. *Can Mineral* 39:341–360
- Brenan JM, McDonough WF, Dalpe C (2003) Experimental constraints on the partitioning of rhenium and some platinum-group elements between olivine and silicate melt. *Earth Planet Sci Lett* 212(1–2):135–150
- Brenan JM, McDonough WF, Ash R (2005) An experimental study of the solubility and partitioning of iridium, osmium and gold between olivine and silicate melt. *Earth Planet Sci Lett* 237(3–4):855–872
- Brenan JM, Finnigan CF, McDonough WF, Homolova V (2012) Experimental constraints on the partitioning of Ru, Rh, Ir, Pt and Pd between chromite and silicate melt: The importance of ferric iron. *Chem Geol* 302–303(0):16–32
- Buchanan DL (1979) A combined transmission electron microscope and electron microprobe study of Bushveld pyroxenes from the Bethal area. *J Petrol* 20:327–354
- Bursztyn NE, Olivo GR (2010) PGE-Rich Ni–Cu sulfide mineralization in the Flin Flon greenstone Belt, Manitoba, Canada: Implications for hydrothermal remobilization of platinum-group elements in basic-ultrabasic sequences. *Econ Geol* 105(8):1469–1490
- Cabral AR, Lehmann B, Kwitko R, Costa CHC (2002) The Serra Pelada Au–Pd–Pt deposit, Carajás Mineral Province, Northern Brazil: reconnaissance mineralogy and chemistry of very high grade palladian gold Mineralization. *Econ Geol* 97(5):1127–1138
- Cabri LJ (2002) The Platinum-Group Minerals. In: Cabri LJ (ed) *Geology, Geochemistry, Mineralogy and Mineral beneficiation of Platinum Group Element*, vol Special Volume 54. Canadian Institute of Mining, Metallurgy and Petroleum, pp 13–129
- Cabri LJ, Blank H, El Goresy A, Laflamme JHG, Nobiling R, Sizgoric MB, Traxel K (1984) Quantitative trace-element analyses of sulfides from Sudbury and Stillwater by proton microprobe. *Can Mineral* 22:521–542
- Campbell IH, Naldrett AJ (1979) The influence of silicate:sulfide ratios on the geochemistry of magmatic sulfides. *Econ Geol* 74:1503–1505
- Campbell IH, Naldrett AJ, Barnes SJ (1983) A model for the origin of the platinum-rich sulfide horizons in the Bushveld and Stillwater Complexes. *J Petrol* 24(2):133–165
- Capobianco CJ, Drake MJ (1990) Partitioning of ruthenium, rhodium, and palladium between spinel and silicate melt and implications for platinum group element fractionation trends. *Geoch Cosmochim Acta* 54(3):869–874
- Capobianco CJ, Hervig RL, Drake MJ (1994) Experiments on crystal/liquid partitioning of Ru, Rh and Pd for magnetite and hematite solid solutions crystallized from silicate melt. *Chem Geol* 113(1–2):23–43
- Causey JD, Galloway JP, Zientek ML (2009) An index to PGE–Ni–Cr deposits and occurrences in selected mineral-occurrence databases. USGS Open-File Report 2009–1045
- Cawthorn RG (1999) The platinum and palladium resources of the Bushveld Complex. *S Afr J Sci* 95(11/12):481
- Cawthorn RG (2002) Platinum-group element deposits in the Bushveld Complex, South Africa. In: Cabri LJ (ed) *Geology, Geochemistry, Mineralogy and Mineral beneficiation of Platinum Group Element*, vol Special Volume 54. Canadian Institute of Mining, Metallurgy and Petroleum, pp 389–429
- Cawthorn RG, Webb SJ (2001) Connectivity between the western and eastern limbs of the Bushveld Complex. *Tectonophysics* 330(3–4):195–209
- Cawthorn RG, Lee CA, Schouwstra RP, Mellowship P (2002) Relationship between PGE and PGM in the Bushveld Complex. *Can Mineral* 40:311–328
- Cawthorn RG, Barnes SJ, Ballhaus C, Malitch KN (2005) Platinum-group element, chromium, and vanadium deposits in mafic and ultramafic rocks. *Eco Geol 100th Anniversary Volume*:215–249



- Chung H-Y, Mungall JE (2009) Physical constraints on the migration of immiscible fluids through partially molten silicates, with special reference to magmatic sulfide ores. *Earth Planet Sci Lett* 286(1–2):14–22
- Cole J, Webb SJ, Finn CA (2014) Gravity models of the Bushveld Complex—have we come full circle? *J Afr Earth Sci* 92:97–118
- Crocket JH (2002) Platinum-group element geochemistry of mafic and ultramafic rocks. In: Cabri LJ (ed) *Geology, Geochemistry, Mineralogy and Mineral beneficiation of Platinum Group Element*, vol Special Volume 54. Canadian Institute of Mining, Metallurgy and Petroleum, pp 553–580
- Czamanske GK, Loferski PJ (1996) Cryptic trace-element alteration of anorthosite, Stillwater Complex, Montana. *Can Mineral* 34:559–579
- Czamanske GK, Zientek GK (1985) *The Stillwater Complex, Montana: geology and guide*. Montana College of Mineral Science and Technology, Butte, Montana
- Dale CW, Macpherson CG, Pearson DG, Hammond SJ, Arculus RJ (2012) Inter-element fractionation of highly siderophile elements in the Tonga Arc due to flux melting of a depleted source. *Geochim Cosmochim Acta* 89(0):202–225
- Davey SR (1992) Lateral variations within the Upper Critical zone of the Bushveld complex on the farm Rooikoppies 297 JQ, Marikana, South Africa. *S Afr J Geol* 95:141–149
- Dubrovsky MI, Rundqvist TV (2009) Petrology of the early Proterozoic platinum-bearing massif of Fedorov Tundra, Kola Peninsula. *Geol Ore Deposits* 51(7):577–587
- Eales HV, Cawthorn RG (1996) The Bushveld Complex. In: Cawthorn RG (ed) *Layered Intrusions*. The Netherlands, Elsevier, Amsterdam, pp 181–230
- Eales HV, Botha WJ, Hattings PJ, de Klerk WJ, Maier WD, Odgers ATR (1993) The mafic rocks of the Bushveld complex: a review of emplacement and crystallization history, and mineralization, in the light of recent data. *J Afr Earth Sci* 16(1–2):121–142
- El-Ghorfi M, Oberthür T, Melcher F, Lüders V, Boukhari A, Maacha L, Ziadi R, Baoutoul H (2006) Gold-palladium mineralization at Bleïda Far West, Bou Azzer-El Graara Inlier, Anti-Atlas, Morocco. *Miner Deposita* 41(6):549–564. doi:10.1007/s00126-006-0077-3
- Evans KA, O'Neill HSC, Mavrogenes JA (2008) Sulfur solubility and sulfide immiscibility in silicate melts as a function of the concentration of manganese, nickel, tungsten and copper at 1 atm and 1400°C. *Chem Geol* 255(1–2):236–249
- Finnigan CS, Brenan JM, Mungall JE, McDonough WF (2008) Experiments and models bearing on the role of chromite as a collector of platinum group minerals by local reduction. *J Petrology*:egn041 doi:10.1093/petrology/egn041
- Fonseca ROC, Campbell IH, O'Neill HSC, Allen CM (2009) Solubility of Pt in sulfide mattes: Implications for the genesis of PGE-rich horizons in layered intrusions. *Geochim Cosmochim Acta* 73(19):5764–5777
- Gain SB (1985) The geologic setting of the platiniferous UG-2 chromitite layer on the farm Maandagshoek, eastern Bushveld Complex. *Econ Geol* 80(4):925–943
- Godel B (2007) *Rôles des liquides sulfurés dans la formation des minéralisations riches en éléments du groupe du platine: applications au complexe du Bushveld (Afrique du Sud) et au complexe de Stillwater (Etats-Unis)* Ph. D. Université du Québec, 369 p
- Godel B (2013) High resolution X-ray computed tomography and its application to ore deposits: case studies from Ni–Cu–PGE deposits. *Econ Geol* 108:2005–2019
- Godel B, Barnes S-J (2008a) Image analysis and composition of platinum-group minerals in the J-M Reef, Stillwater Complex (U.S.A.). *Econ Geol* 103(3):637–651
- Godel B, Barnes S-J (2008b) Platinum-group elements in sulfide minerals and the whole rocks of the J-M Reef (Stillwater Complex): implication for the formation of the reef. *Chem Geol* 248:272–294
- Godel B, Barnes S-J, Maier WD (2006) 3-D distribution of sulfide minerals in the Merensky Reef (Bushveld Complex, South Africa) and the J-M Reef (Stillwater Complex, USA) and their relationship to microstructures using X-Ray Computed Tomography. *J Petrol* 47:1853–1872
- Godel B, Barnes S-J, Maier WD (2007) Platinum-group elements in sulfide minerals, platinum-group minerals, and whole-rocks of the Merensky Reef (Bushveld Complex, South Africa): Implications for the formation of the reef. *J Petrol* 48(8):1569–1604



- Godel B, Maier WD, Barnes S-J (2008) Platinum-group elements in the Merensky and J-M Reefs: a review of recent studies. *J Geol Soc India* 72:595–609
- Godel B, Barnes SJ, Barnes S-J, Maier WD (2010) Platinum ore in 3D: Insights from high-resolution X-ray computed tomography. *Geology* 38(12):1127–1130
- Godel B, Barnes S-J, Maier WD (2011) Parental magma composition inferred from trace element in cumulus and intercumulus silicate minerals: an example from the Lower and Lower Critical Zones of the Bushveld Complex, South Africa. *Lithos* 125:537–552
- Godel B, Rudashevsky NS, Nielsen TFD, Barnes SJ, Rudashevsky VN (2014) Constraints on the origin of the Skaergaard intrusion mineralization: insights from high-resolution X-ray computed tomography. *Lithos* 190(27–36)
- Halkoaho TAA, Alapieti TT, Lahtinen JJ (1990) The Sompujarvi PGE reef in the Penikat layered intrusion, northern Finland. *Miner Petrol* 42(1–4):39–55. doi:10.1007/bf01162683
- Hamlyn PR, Keays RR (1986) Sulfur saturation and second stage melts: application to the Bushveld platinum metal deposits. *Econ Geol* 81:1431–1435
- Hanley JJ (2005) The aqueous geochemistry of the platinum-group elements (PGE) in surficial, low-T hydrothermal and high-T magmatic-hydrothermal environments. In: Mungall JE (ed) *Exploration for platinum-group element deposits*, vol Short Course 35. Mineralogical Association of Canada, pp 35–56
- Hanley JJ, Pettke T, Mungall JE, Spooner ETC (2005) The solubility of platinum and gold in NaCl brines at 1.5 kbar, 600 to 800[deg]C: A laser ablation ICP-MS pilot study of synthetic fluid inclusions. *Geoch Cosmochim Acta* 69(10):2593–2611
- Hiemstra SA (1979) The role of collectors in the formation of the platinum deposits in the Bushveld Complex. *Can Mineral* 17:469–482
- Hiemstra SA (1986) The distribution of chalcophile and platinum-group elements in the UG-2 chromitite layer of the Bushveld Complex. *Econ Geol* 81(5):1080–1086
- Hirschmann MM, Renne PR, McBirney AR (1997) <sup>40</sup>Ar/<sup>39</sup>Ar dating of the Skaergaard intrusion. *Earth Planet Sci Lett* 146(3–4):645–658
- Holness MB, Tegner C, Nielsen TFD, Stripp G, Morse SA (2007) A textural record of solidification and cooling in the Skaergaard Intrusion, East Greenland. *J Petrology*:egm064 doi:10.1093/petrology/egm064
- Holwell DA, Keays RR (2014) The Formation of Low-Volume, High-Tenor Magmatic PGE-Au Sulfide Mineralization in Closed Systems: Evidence from Precious and Base Metal Geochemistry of the Platinova Reef, Skaergaard Intrusion, East Greenland. *Econ Geol* 109(2):387–406
- Holwell D, McDonald I (2006) Petrology, geochemistry and the mechanisms determining the distribution of platinum-group element and base metal sulfide mineralisation in the Platreef at Overysel, northern Bushveld Complex, South Africa. *Miner Deposita* 41:575–598
- Holwell DA, McDonald I (2007) Distribution of platinum-group elements in the Platreef at Overysel, northern Bushveld Complex: a combined PGM and LA-ICP-MS study. *Contrib Mineral Petrol* 154(2):171–190
- Holwell DA, McDonald I, Armitage PEB (2006) Platinum-group mineral assemblages in the Platreef at the Sandsloot Mine, northern Bushveld Complex, South Africa. *Mineral Mag* 70(1):83–101
- Holwell DA, Boyce AJ, McDonald I (2007) Sulfur isotope variations within the Platreef Ni–Cu–PGE Deposit: genetic implications for the origin of sulfide mineralization. *Econ Geol* 102(6):1091–1110
- Huhtelin TA, Alapieti TT, Lahtinen JJ (1990) The Paasivaara PGE reef in the Penikat layered intrusion, northern Finland. *Mineral Petrol* 42(1–4):57–70
- Hutchinson D, Kinnaird JA (2005) Complex multistage genesis for the Ni–Cu–PGE mineralisation in the southern region of the Platreef, Bushveld Complex, South Africa. *Applied Earth Sc* 114
- Hutchinson D, McDonald I (2008) Laser ablation ICP-MS study of platinum-group elements in sulfides from the Platreef at Turfspruit, northern limb of the Bushveld Complex, South Africa. *Miner Deposita* 43(6):695–711
- Jenner FE, O'Neill HSC, Arculus RJ, Mavrogenes JA (2010) The magnetite crisis in the evolution of arc-related magmas and the initial concentration of Au, Ag and Cu. *J Petrol* 51(12):2445–2464
- Johnson-Matthey (2011) *Platinum 2011 Interim Review*. (40)

- Jugo PJ (2009) Sulfur content at sulfide saturation in oxidized magmas. *Geology* 37(5):415–418
- Jugo PJ, Luth RW, Richards JP (2005) An experimental study of the sulfur content in basaltic melts saturated with immiscible sulfide or sulfate liquids at 1300C and 10 GPa. *J Petrol* 46(4):783–798
- Kanitpanyacharoen W, Boudreau AE (2013) Sulfide-associated mineral assemblages in the Bushveld Complex, South Africa: platinum-group element enrichment by vapor refining by chloride-carbonate fluids. *Miner Deposita* 48(2):193–210
- Keays R, Lightfoot P, Hamlyn P (2012) Sulfide saturation history of the Stillwater Complex, Montana: chemostratigraphic variation in platinum group elements. *Miner Deposita* 47(1–2):151–173
- Kerr A, Leitch AM (2005) Self-destructive sulfide segregation systems and the formation of high-grade magmatic deposits. *Econ Geol* 100:311–332
- Kingston GA, El-Dosuky BT (1982) A contribution on the platinum-group mineralogy of the Merensky Reef at the Rustenburg Platinum Mine. *Econ Geol* 77(6):1367–1384
- Kinloch ED (1982) Regional Trends in the Platinum-Group Mineralogy of the Critical Zone of the Bushveld Complex, South-Africa. *Econ Geol* 77(6):1328–1347
- Kinloch ED, Peyerl W (1990) Platinum-group minerals in various rock types of the Merensky Reef: Genetic Implications. *Econ Geol* 85:537–555
- Kinnaird J, Hutchinson D, Schurmann L, Nex P, de Lange R (2005) Petrology and mineralisation of the southern Platreef: northern limb of the Bushveld Complex, South Africa. *Miner Deposita* 40(5):576–597
- Kogiso T, Suzuki K, Suzuki T, Shinotsuka K, Uesugi K, Takeuchi A, Suzuki Y (2008) Detecting micrometer-scale platinum-group minerals in mantle peridotite with microbeam synchrotron radiation X-ray fluorescence analysis. *Geochem Geophys Geosyst* 9(3):Q03018
- Kruger F (2005) Filling the Bushveld Complex magma chamber: lateral expansion, roof and floor interaction, magmatic unconformities, and the formation of giant chromitite, PGE and Ti-V-magnetite deposits. *Miner Deposita* 40(5):451–472
- Latypov R, O'Driscoll B, Lavrenchuk A (2013) Towards a model for the in situ origin of PGE reefs in layered intrusions: insights from chromitite seams of the Rum Eastern Layered Intrusion, Scotland. *Contrib Mineral Petrol* 166(1):309–327
- Laurenz V, Fonseca RIOC, Ballhaus C, Jochum KP, Heuser A, Sylvester PJ (2013) The solubility of palladium and ruthenium in picritic melts: 2. The effect of sulfur. *Geochim Cosmochim Acta* 108:172–183
- Lavigne MJ, Michaud MJ (2001) Geology of the North American Palladium Ltd's Roby zone deposit, Lac des Iles. *Exploration and Mining geology* 10:1–17
- Lechler PJ, Arehart GB, knight M (2002) Multielement and isotopic geochemistry of the J-M Reef, Stillwater Intrusion, Montana. In: 9th International Platinum symposium, vol Abstract Programm. Billings, pp 245–248
- Lee CA (1996) A review of mineralization in the Bushveld Complex and some other layered intrusions. In: Cawthorn RG (ed) *Layered Intrusions*. Elsevier, Amsterdam, pp 103–145
- Lee CA, Parry SJ (1988) Platinum-Group Element geochemistry of the lower and middle group chromitites of the eastern Bushveld Complex. *Econ Geol* 83(6):1127–1139
- Li C, Ripley EM (2005) Empirical equations to predict the sulfur content of mafic magmas at sulfide saturation and applications to magmatic sulfide deposits. *Miner Deposita*:46
- Li C, Ripley EM (2006) Formation of Pt–Fe alloy by desulfurization of Pt–Pd sulfide in the J-M Reef of the Stillwater Complex, Montana. *Can Mineral* 44:895–903
- Li C, Ripley EA (2009) Sulfur contents at sulfide-liquid or anhydrite saturation in silicate melts: empirical equations and example applications. *Econ Geol* 104:405–412
- Li C, Ripley EM, Merino E, Maier WD (2004) Replacement of base metal sulfides by actinolite, epidote, calcite, and magnetite in the UG2 and Merensky Reef of the Bushveld Complex, South Africa. *Econ Geol* 99(1):173–184
- Liu Y, Samaha N-T, Baker DR (2007) Sulfur concentration at sulfide saturation (SCSS) in magmatic silicate melts. *Geochim Cosmochim Acta* 71(7):1783–1799
- Loemelis M, Melcher F, Oberthür T (2010) Platinum-group element distribution in the oxidized Main Sulfide Zone, Great Dyke, Zimbabwe. *Miner Deposita* 45(1):93–109. doi:10.1007/s00126-009-0258-y

- Loemelis M, Pearson NJ, Barnes SJ, Fiorentini ML (2011) Ruthenium in komatiitic chromite. *Geochim Cosmochim Acta* 75(13):3645–3661
- Lorand J-P, Alard O (2001) Platinum-group element abundances in the upper mantle: new constraints from in situ and whole-rock analyses of Massif Central xenoliths (France). *Geochim Cosmochim Acta* 65(16):2789–2806
- Lorand J-P, Luguët A, Alard O, Bezos A, Meisel T (2008a) Abundance and distribution of platinum-group elements in orogenic lherzolites; a case study in a Fontete Rouge lherzolite (French Pyrenees). *Chem Geol* 248(3–4):174–194
- Lorand JP, Luguët A, Alard O (2008b) Platinum-group elements: a new set of key tracers for the Earth's interior. *Elements* 4:247–252
- Lorand J-P, Alard O, Luguët A (2010) Platinum-group element micronuggets and refertilization process in Lherz orogenic peridotite (northeastern Pyrenees, France). *Earth Planet Sci Lett* 289:298–310
- Luguët A, Shirey SB, Lorand J-P, Horan MF, Carlson RW (2007) Residual platinum-group minerals from highly depleted harzburgites of the Lherz massif (France) and their role in HSE fractionation of the mantle. *Geochim Cosmochim Acta* 71:1553–1570
- Maier WD (2005) Platinum-group element (PGE) deposits and occurrences: Mineralization styles, genetic concepts, and exploration criteria. *J Afr Earth Sci* 41:165–191
- Maier WD, Barnes SJ (1999) Platinum-group elements in silicate rocks of the Lower, Critical and Main Zones at union section, western Bushveld Complex. *J Petrol* 40(11):1647–1671
- Maier WD, Barnes S-J (2008) Platinum-group elements in the UG1 and UG2 chromitites, and the Bastard reef, at Impala platinum mine, western Bushveld Complex, South Africa: Evidence for late magmatic cumulate instability and reef constitution. *S Afr J Geol* 111:159–176
- Maier W, Groves D (2011) Temporal and spatial controls on the formation of magmatic PGE and Ni–Cu deposits. *Miner Deposita* 46(8):841–857
- Maier WD, Barnes SJ, Gartz V, Andrews G (2003) Pt–Pd reefs in magnetites of the Stella layered intrusion, South Africa: A world of new exploration opportunities for platinum group elements. *Geology* 31(10):885–888
- Maier WD, Barnes SJ, Bandyayera D, Livesey T, Li C, Ripley E (2008) Early Kibaran rift-related mafic-ultramafic magmatism in western Tanzania and Burundi: Petrogenesis and ore potential of the Kapalagulu and Musongati layered intrusions. *Lithos* 101(1–2):24–53
- Maier WD, Barnes SJ, Groves DI (2013) The Bushveld Complex, South Africa: formation of platinum, palladium, chrome- and vanadium-rich layers via hydrodynamic sorting of a mobilized cumulate slurry in a large, relatively slowly cooling, subsiding magma chamber. *Miner Deposita* 48(1):1–56
- Manyeruke TD, Maier WD, Barnes S-J (2005) Major and trace element geochemistry of the Platreef on the farm Townlands, northern Bushveld Complex. *S Afr J Geol* 108(3):381–396
- Mavrogenes JA, O'Neill HSC (1999) The relative effects of pressure, temperature and oxygen fugacity on the solubility of sulfide in mafic magmas. *Geochim Cosmochim Acta* 63(7–8):1173–1180
- McBirney AR (1996) The Skaergaard intrusion. In: Cawthorn RG (ed) *Layered intrusions*. Elsevier, Amsterdam, pp 174–180
- McCallum IS, Raedeke LD, Mathez EA (1980) Investigations of the Stillwater Complex: Part I. Stratigraphy and Structure of the Banded Zone. *Am J Sci* 280-A:59–87
- McCandless TE, Ruiz J (1991) Osmium isotopes and crustal sources for platinum-group mineralization in the Bushveld Complex, South africa. *Geology* 19:1225–1228
- McDonald I, Holwell DA (2011) Geology of the Northern Bushveld Complex and the Setting and Genesis of the Platreef Ni–Cu–PGE Deposit. *Reviews in. Econ Geol* 17:297–327
- McDonough WF, Sun SS (1995) The composition of the Earth. *Chem Geol* 120:223–253
- McLaren CH, De Villiers JPR (1982) The Platinum-Group Chemistry and Mineralogy of the UG-2 Chromitite Layer of the Bushveld Complex. *Econ Geol* 77:1348–1366
- Miller JD, Green JC, Severson MJ, Chandler VW, Hauck SA, Peterson DM, Wahl TE (2002) Geology and mineral potential of the Duluth Complex and related rocks of northeastern Minnesota. *Minnesota Geological survey Report of Investigations* 58:207

- Molnar F, Watkinson dH, Jones PC (2001) Multiple hydrothermal processes in footwall units of the North Range, subvolcanic Igneous Complex, Canada, and implications for the genesis of vein-type Cu–Ni–PGE deposits. *Econ Geol* 96:1645–1670
- Mondal SK, Mathez EA (2007) Origin of the UG2 chromitite layer, Bushveld Complex. *J Petrol* 48(3):495–510
- Moroni M, Girardi V, Ferrario A (2001) The Serra Pelada Au–PGE deposit, Serra dos Carajás (Pará State, Brazil): geological and geochemical indications for a composite mineralising process. *Miner Deposita* 36(8):768–785
- Mungall JE (2002a) Kinetic controls on the partitioning of trace elements between silicate and sulfide liquids. *J Petrol* 43(5):749–768
- Mungall JE (2002b) Roasting the mantle: slab melting and the genesis of major Au and Au-rich Cu deposits. *Geology* 30:915–918
- Mungall JE (2007) Magmatic ore deposits. In: Holland HD, Turekian KK (eds) *Treatise on Geochemistry*, vol 3. Pergamon, Oxford, pp 1–33
- Mungall JE (2014) Geochemistry of Magmatic ore deposits. In: Holland HD, Turekian KK (eds) *Treatise on Geochemistry*, vol 13. Pergamon, Oxford, pp 195–218
- Mungall JE, Brenan JM (2014) Partitioning of platinum-group elements and Au between sulfide liquid and basalt and the origins of mantle-crust fractionation of the chalcophile elements. *Geochim Cosmochim Acta* 125(0):265–289
- Mungall JE, Naldrett A (2008) Ore deposits of the platinum-group elements. *Elements* 4:253–258
- Mungall JE, Su S (2005) Interfacial tension between magmatic sulfide and silicate liquids: Constraints on kinetics of sulfide liquation and sulfide migration through silicate rocks. *Earth Planet Sc Lett* 234(1–2):135–149
- Mungall JE, Hanley JJ, Arndt NT, Debecdelievre A (2006) Evidence from meimechites and other low-degree mantle melts for redox controls on mantle-crust fractionation of platinum-group elements. *Proc Natl Acad Sci* 103(34):12695–12700
- Mutanen T (1997) Geology and petrology of the Akanvaara and Koitelainen mafic layered intrusion and Keivitsa-Satovaara layered Complex, northern Finland. Geological Survey of Finland Field Trip Guidebook, 10th International Platinum Symposium Bulletin 395:233
- Naldrett AJ (2004) *Magmatic sulfide deposits; geology, geochemistry and exploration*. Berlin, Springer Verlag, Germany,
- Naldrett A (2011) Fundamentals of magmatic sulfide deposits. *Reviews in. Econ Geol* 17:1–50
- Naldrett AJ, Gasparrini EC, Barnes SJ, Von Gruenewaldt G, Sharpe MR (1986) The Upper Critical Zone of the Bushveld Complex and the origin of Merensky-type ores. *Econ Geol* 81(5):1105–1117
- Naldrett AJ, Kinnaird J, Wilson A, Yudovskaya M, McQuade S, Chunnett G, Stanley C (2009a) Chromite composition and PGE content of Bushveld chromitites: Part 1 and 2; the Lower and Middle Groups. *Appl Earth Sci* 118(3–4):131–161
- Naldrett AJ, Wilson A, Kinnaird J, Chunnett G (2009b) PGE tenor and metal ratios within and below the Merensky Reef, Bushveld Complex: Implications for its Genesis. *J Petrology*:egp015 doi:10.1093/petrology/egp015
- Naldrett A, Kinnaird J, Wilson A, Yudovskaya M, Chunnett G (2011a) Genesis of PGE-enriched Merensky Reef and chromitite seams of the Bushveld Complex. *Reviews in. Econ Geol* 17:235–296
- Naldrett A, Wilson A, Kinnaird J, Yudovskaya M, Chunnett G (2011b) The origin of chromitites and related PGE mineralization in the Bushveld Complex: new mineralogical and petrological constraints. *Miner Deposita*:1–24
- Naldrett A, Wilson A, Kinnaird J, Yudovskaya M, Chunnett G (2012) The origin of chromitites and related PGR mineralization in the Bushveld Complex: new mineralogical and petrological constraints. *Miner Deposita* 47:209–232
- Nielsen TFD (1975) Possible mechanism of continental break-up in the North Atlantic. *Nature* 253:182–184
- Nielsen TFD (2001) The palladium potential of the skaergaard intrusion, South-East Greenland. *Danmarks og Grønlands Geologiske Undersøgelse Rapport 2002/113*:39

- Nielsen TFD (2004) The Shape and Volume of the Skaergaard Intrusion, Greenland: Implications for Mass Balance and Bulk Composition. *J Petrol* 45(3):507–530
- Nielsen TFD, Andersen JCO, Brook CK (2005) The Platinova Reef of the Skaergaard Intrusion. In: Mungall JE (ed) *Exploration for Platinum-Group Element Deposits*, vol 35. Mineralogical Association of Canada, pp 431–456
- Nunes PD, Tilton GR (1971) Uranium-lead ages of minerals from the Stillwater Complex and associated rocks, Montana. *Geol Soc Am Bull* 82:2231–2250
- Oberthür T (2002) Platinum-group element mineralization of the Great Dyke, Zimbabwe. *Geology, Geochemistry, Mineralogy and Mineral beneficiation of Platinum Group Element Special Volume* 54:483–506
- Oberthür T (2011) Platinum-group element mineralization of the Main Sulphide Zone, Great Dyke, Zimbabwe. *Reviews in. Econ Geol* 17:329–350
- Oberthür T, Melcher F (2005) Behaviour of platinum-group elements and platinum-group minerals in the superegene environment: a caase study of persistence and redistribution in the Main Sulphide Zone of the Great Dyke, Zimbabwe. In: Mungall JE (ed) *Exploration for Platinum-Group Elements Deposits*, vol Short Course Vol. 35. Mineralogical Association of Canada, pp 97–111
- Oberthür T, Davis DW, Blenkinsop TG, Hohndorf A (2002) Precise U–Pb mineral ages, Rb–Sr and Sm–Nd systematics for the Great Dyke, Zimbabwe—constraints on late Archean events in the Zimbabwe craton and Limpopo belt. *Precambrian Res* 113(3):293–305
- Oberthür T, Weiser T, Gast L (2003) Geochemistry and mineralogy of platinum-group elements at Hartley Platinum Mine, Zimbabwe. *Mineral Deposita* 344–355
- Olivo GR, Gauthier M, Williams-Jones AE, Levesque M (2001) The Au–Pd Mineralization at the Conceicao Iron Mine, Itabira District, Southern Sao Francisco Craton, Brazil: an example of a Jacutinga-type deposit. *Econ Geol* 96(1):61–74
- Olsson JR, Soderlund U, Klausen MB, Ernst RE (2010) U–Pb baddeleyite ages linking major Archean dyke swarms to volcanic-rift forming events in the Kaapvaal craton (South Africa), and a precise age for the Bushveld Complex. *Precambrian Res* 183(3):490–500
- Osbah I (2012) Platinum-group element distribution in base-metal sulfides of the Merensky Reef and UG2 from the eastern and western Bushveld Complex, South Africa. Ph. D. Friedrich-Alexander Universität Erlangen-Nürnberg
- Osbah I, Klemd R, Oberthür T, Brätz H, Schouwstra R (2013) Platinum-group element distribution in base-metal sulfides of the Merensky Reef from the eastern and western Bushveld Complex, South Africa. *Miner Deposita* 48(2):211–232
- Page NJ (1976) Serpentinization and alteration in an olivine cumulate from the Stillwater Complex, southwestern Montana. *Contrib Mineral Petrol* 54:127–137
- Page NJ (1977) Stillwater Complex, Montana: rock succession, metamorphism and structure of the complex and adjacent rocks. US Geological Survey Professional paper, 999:79
- Page NJ, Zientek ML (1985) Geologic and Structural setting of the Stillwater Complex. In: Czamanske GK, Zientek ML (eds) *The Stillwater Complex, Montana: geology and guide*, vol Special Publication, no. 92. Montana Bureau of Mines and Geology, Butte, Montana, pp 1–8
- Pagé P, Barnes S-J, Bédard JH, Zientek ML (2012) In situ determination of Os, Ir, and Ru in chromites formed from komatiite, tholeiite and boninite magmas: Implications for chromite control of Os, Ir and Ru during partial melting and crystal fractionation. *Chem Geol* 302–303(0):3–15
- Park J-W, Campbell IH, Arculus RJ (2013) Platinum-alloy and sulfur saturation in an arc-related basalt to rhyolite suite: Evidence from the Pual Ridge lavas, the Eastern Manus Basin. *Geochim Cosmochim Acta* 101(0):76–95
- Penniston-Dorland SC, Wing BA, Nex PAM, Kinnaird JA, Farquhar J, Brown M, Sharman ER (2008) Multiple sulfur isotopes reveal a magmatic origin for the Platereef platinum group element deposit, Bushveld Complex, South Africa. *Geology* 36(12):979–982
- Peregoedova A, Barnes S-J, Baker DR (2004) The formation of Pt–Ir alloys and Cu–Pd-rich sulfide melts by partial desulfurization of Fe–Ni–Cu sulfides: results of experiments and implications for natural systems. *Chem Geol* 208(1–4):247–264
- Peregoedova A, Barnes S-J, Baker DR (2006) An experimental study of mass transfer of platinum-group elements, gold, nickel and copper in sulfur-dominated vapor at magmatic temperatures. *Chem Geol* 235(1–2):59–75



- Polovina JS, Hudson DM, Jones RE (2004) Petrographic and geochemical characteristics of post-magmatic hydrothermal alteration and mineralization in the J-M Reef, Stillwater Complex, Montana. *Can Mineral* 42:261–277
- Premo WR, Helz RT, Zientek ML, Langston RB (1990) U–Pb and Sm–Nd ages for the Stillwater Complex and its associated sills and dikes, Beartooth Mountains, Montana: Identification of a parent magma? *Geology* 18:1065–1068
- Prendergast MD (2000) Layering and precious metals mineralization in the Rincon del Tigre Complex, Eastern Bolivia. *Econ Geol* 95:113–130
- Prichard HM, Barnes S-J, Maier WD, Fisher PC (2004) Variations in the nature of the platinum-group minerals in a cross-section through the Merensky Reef at Impala Platinum: Implications for the mode of formation of the reef. *Can Mineral* 42:423–437
- Puchtel I, Humayun M (2000) Platinum group elements in Kostomuksha komatiites and basalts: implications for oceanic crust recycling and core-mantle interaction. *Geochim Cosmochim Acta* 64(24):4227–4242
- Raedeker LD, McCallum SI (1984) Investigations in the Stillwater Complex: Part II. Petrology and Petrogenesis of the Ultramafic Series. *J Petrol* 25:395–420
- Richardson SH, Shirey SB (2008) Continental mantle signature of Bushveld magmas and coeval diamonds. *Nature* 453(7197):910–913
- Righter K, Campbell AJ, Humayun M, Hervig RL (2004) Partitioning of Ru, Rh, Pd, Re, Ir, and Au between Cr-bearing spinel, olivine, pyroxene and silicate melts. *Geochim Cosmochim Acta* 68(4):867–880
- Ripley E, Li C (2013) Sulfide saturation in mafic magmas: is external sulfur required for magmatic Ni–Cu–(PGE) ore genesis? *Econ Geol* 108:45–58
- Rudashevsky NS, McDonald AM, Cabri LJ, Nielsen TFD, Stanley CJ, Kretzer YL, Rudashevsky VN (2004) Skaergaardite, PdCu, a new platinum-group intermetallic mineral from the Skaergaard intrusion, Greenland. *Mineral Mag* 68(4):615–632
- Rudashevsky NS, Kretzer YL, Rudashevsky VN, Nielsen TFD (2009) Gold, PGE and sulfide phases of the precious mineralization of the Skaergaard intrusion, parts 6 and 7. *Danmarks og Grønlands Geologiske Undersøgelse Rapport 2009* 54 and 68:33 p
- Sa JHS, Barnes S-J, Prichard HM, Fisher PC (2005) The distribution of base metals and platinum-group elements in magnetitite and its host rocks in the Rio Jacare Intrusion, northeastern Brazil. *Econ Geol* 100(2):333–348
- Sattari P, Brennan JM, Horn I, McDonough WF (2002) Experimental Constraints on the Sulfide- and Chromite- Silicate Melt Partitioning Behavior of Rhenium and Platinum-Group Elements. *Econ Geol* 97(2):385–398
- Sharman ER, Penniston-Dorland SC, Kinnaird JA, Nex PAM, Brown M, Wing BA (2013) Primary origin of marginal Ni–Cu–(PGE) mineralization in layered intrusions:  $\Delta 33\text{S}$  evidence from the Platreef, Bushveld, South Africa. *Econ Geol* 108(2):365–377
- South African Committee For Stratigraphy (1980) Stratigraphy of Southern Africa. Part 1. Lithostratigraphy of South Africa, South West/ Namibia, and the Republics of the Boputhatswana, Trankei, and Venda. In: *Geological Survey of South Africa Handbook*, vol 8. p 690
- Teigler B, Eales HV (1993) Correlation between chromite composition and PGE mineralization in the critical zone of the western Bushveld Complex. *Miner Deposita* 28(5):291–302
- Todd SG, Keith DW, Le Roy LW, Schissel DJ, Mann EL, Irvine TN (1982) The J-M platinum-palladium reef of the Stillwater Complex, Montana: I. stratigraphy and petrology. *Econ Geol* 77:1145–1180
- Turner AR, Wolfgram D, Barnes SJ (1985) Geology of the Stillwater County sector of the J-M Reef, including the Minneapolis Adit. In: Czamanske GK, Zientek ML (eds) *The Stillwater Complex, Montana: geology and guide*, vol Special Publication, no. 92. Montana Bureau of Mines and Geology, Butte, Montana, pp 210–230
- van der Merwe F, Viljoen F, Knoper M (2012) The mineralogy and mineral associations of platinum group elements and gold in the Platreef at Zwartfontein, Akanani Project, Northern Bushveld Complex, South Africa. *Mineral Petrol* 106(1–2):25–38

- Vermaak CF (1976) Merensky Reef—Thoughts on Its Environment and Genesis. *Econ Geol* 71(7):1270–1298
- Vermaak CF, Hendriks LP (1976) A review of the mineralogy of the Merensky Reef, with specific reference to new data on the precious metal mineralogy. *Econ Geol* 71(7):1244–1269
- Viljoen MJ (1999) The nature and origin of the Merensky Reef of the western Bushveld Complex based on geological facies and geophysical data. *South Afr J Geol* 102(3):221–239
- Von Gruenewaldt G (1979) A review of some recent concepts of the Bushveld Complex, with particular reference to sulfide mineralization. *Canadian mineralogist* 17:233–256
- Von Gruenewaldt G (1986) Platinum-group element-chromitite associations in the Bushveld Complex. *Econ Geol* 81:1067–1079
- Von Gruenewaldt G, Horsch H, Dickst D, de Wet J (1990) PGE mineralization in the western sector of the eastern Bushveld Complex. *Mineral Petrol* 42(1–4):71–95
- Vukmanovic Z, Barnes SJ, Reddy S, Godel B, Fiorentini ML (2013) Microstructure in chromite crystals of the Merensky Reef (Bushveld Complex, South Africa). *Contrib Mineral Petrol* 165(6):1031–1050
- Wager LR, Brown GM (1968) Layered igneous rocks. Oliver and Boyd, Edinburgh
- Webb SJ, Cawthorn KG, Nguuri T, James D (2004) Gravity modeling of Bushveld Complex connectivity supported by Southern African Seismic Experiment results. In: *South Afr J Geol*, vol 107. Geological Society of South Africa, pp 207–218
- Wendlandt RF (1982) Sulfide saturation of basalt and andesite melts at high pressures and temperatures. *Am Mineral* 67(9–10):877–885
- Willmore CC, Boudreau AE, Kruger FJ (2000) The halogen geochemistry of the Bushveld Complex, Republic of South Africa: Implications for chalcophile element distribution in the lower and critical zones. *J Petrol* 41(10):1517–1539
- Wilson AH (1982) The Geology of the Great Dyke, Zimbabwe: The Ultramafic Rocks. *J Petrol* 23(2):240–292
- Wilson A (1996) The great Dyke of Zimbabwe. In: Cawthorn RG (ed) *Layered Intrusions*, vol. Elsevier Science, Amsterdam, pp 365–402
- Wilson AH (2012) A chill sequence to the Bushveld Complex: insight into the first stage of emplacement and implications for the parental magmas. *J Petrol* 53(6):1123–1168
- Wilson AH, Chunnett G (2006) Trace element and platinum group element distributions and the genesis of the Merensky Reef, Western Bushveld Complex, South Africa. *J Petrol* 47:2369–2403
- Wilson AH, Prendergast MD (1989) The Great dyke of Zimbabwe—I: tectonic setting, stratigraphy, petrology, structure, emplacement and crystallization. In: Prendergast MD, Jones MJ (eds) *Magmatic sulfides—The Zimbabwe Volume*, vol. The Institution of Mining and Metallurgy, London, pp 1–20
- Wilson AH, Prendergast MD (2001) Platinum-group element mineralisation in the Great Dyke, Zimbabwe, and its relationship to magma evolution and magma chamber structure. *South Afr J Geol* 104:319–342
- Wilson AH, Tredoux M (1990) Lateral and vertical distribution of platinum-group elements and petrogenetic controls on the sulfide mineralization in the P1 pyroxenite layer of the Darwendale Subchamber of the Great Dyke, Zimbabwe. *Econ Geol* 85:556–584
- Wohlgemuth-Ueberwasser C, Fonseca R, Ballhaus C, Berndt J (2013) Sulfide oxidation as a process for the formation of copper-rich magmatic sulfides. *Miner Deposita* 48:115–127
- Wood SA (2002) The aqueous Geochemistry of the platinum-group elements with applications to ore deposits. In: Cabri LJ (ed) *Geology, Geochemistry, Mineralogy and Mineral beneficiation of Platinum Group Element*, vol Special Volume 54. Canadian Institute of Mining, Metallurgy and Petroleum, pp 211–249
- Worst BG (1960) The great Dyke of Southern Rhodesia. *South Rhod Geol Surv Bull* 47:234
- Yudovskaya M, Kinnaird J, Naldrett AJ, Mokhov AV, McDonald I, Reinke C (2012) Facies variation in PGE mineralization in the central Platreef of the Bushveld Complex, South Africa. *Can Mineral* 49(6):1349–1384



- Zientek ML, Czamanske GK, Irvine TN (1985) Stratigraphy and nomenclature for the Stillwater Complex. In: Czamanske GK, Zientek ML (eds) *The Stillwater Complex, Montana: geology and guide*, vol Special Publication, no. 92. Montana Bureau of Mines and Geology, Butte, Montana, pp 21–32
- Zientek ML, Cooper RW, Corson SR, Geraghty EP (2002) Platinum-group element mineralization in the Stillwater Complex, Montana. In: Cabri LJ (ed) *Geology, Geochemistry, Mineralogy and Mineral beneficiation of Platinum Group Element*, vol Special Volume 54. Canadian Institute of Mining, Metallurgy and Petroleum, pp 459–481